Introduction of Unsaturation into the *N-n*-Alkyl Chain of the Nicotinic Receptor Antagonists, NONI and NDNI: Effect on Affinity and Selectivity

Sangeetha P. Sumithran,[1] Peter A. Crooks,[1] Rui Xu,[1,2] Jun Zhu,[1] Agripina G. Deaciuc,[1] Lincoln H. Wilkins,[1,3] and Linda P. Dwoskin[1]

[1] College of Pharmacy, University of Kentucky, Lexington, KY 40536-0082

[2] Current address: Array BioPharma, Boulder, CO 80301

[3] Current address: Bristol-Myers Squibb, New Orleans, LA 70433

ABBREVIATIONS: ANOVA, analysis of variance; BSA, bovine serum albumin; DA, dopamine; DAT, dopamine transporter; HEPES, N-[2-hydroxyethyl] piperazine-N'-[2-ethanesulfonic acid]; MLA, methyllycaconitine; nAChR, neuronal nicotinic acetylcholine receptor; NDNI, *N-n*-decylnicotinium iodide; NDNB4c, *N-cis-n*-dec-4-enyl nicotinium bromide; NDNB4t, *N-trans-n*-dec-4-enylnicotinium bromide; NDNB9e, *N-n*-dec-9-enylnicotinium bromide; NDNB3y, *N-n*-dec-3-ynylnicotinium bromide; NONB3c, *N-cis-n*-oct-3-enylnicotinium bromide; NONB3t, *N-trans-n*-oct-3-enylnicotinium bromide; NONB7e, *N-n*-oct-7-enylnicotinium bromide; NONB3y, *N-n*-oct-3-ynylnicotinium bromide; NONI, *N-n*-octylnicotinium iodide; PEI, polyethylenimine; S.E.M., standard error of the mean; * indicates putative nAChR subtype assignment.

ABSTRACT

N-n-Octylnicotinium iodide (NONI) and *N-n*-decylnicotinium iodide (NDNI) are selective nicotinic receptor (nAChR) antagonists mediating nicotine-evoked striatal dopamine (DA) release, and inhibiting [³H]nicotine binding, respectively. This study evaluated effects of introducing unsaturation into the *N-n*-alkyl chains of NONI and NDNI on inhibition of [³H]nicotine and [³H]methyllycaconitine binding ($\alpha4\beta2*$ and $\alpha7*$ nAChRs, respectively), $^{86}Rb^+$ efflux and [³H]DA release (agonist or antagonist effects at $\alpha4\beta2*$ and $\alpha6\beta2*$-containing nAChRs, respectively). In the NONI series, introduction of a C_3-*cis*- (NONB3c), C_3-*trans*- (NONB3t), C_7-double-bond (NONB7e), or C_3-triple-bond (NONB3y) afforded a 4-fold to 250-fold increased affinity for [³H]nicotine binding sites compared with NONI. NONB7e and NONB3y inhibited nicotine-evoked $^{86}Rb^+$ efflux, indicating $\alpha4\beta2*$ antagonism. NONI analogs exhibited a 3-fold to 8-fold greater potency inhibiting nicotine-evoked [³H]DA overflow compared with NONI (IC_{50} = 0.62 μM; Imax = 89%), with no change in Imax, except for NONB3y (Imax = 50%). In the NDNI series, introduction of

a C_4-*cis*- (NDNB4c), C_4-*trans*-double-bond (NDNB4t), or C_3-triple-bond (NDNB3y) afforded a 4-fold to 80-fold decreased affinity for [³H]nicotine binding sites compared with NDNI, whereas introduction of a C_9 double-bond (NDNB9e) did not alter affinity. NDNB3y and NDNB4t inhibited nicotine-evoked $^{86}Rb^+$ efflux, indicating antagonism at $\alpha4\beta2*$ nAChRs. Although NDNI had no effect, NDNB4t and NDNB9e potently inhibited nicotine-evoked [³H]DA overflow (IC_{50} = 0.02–0.14 μM, Imax = 90%), as did NDNB4c (IC_{50} = 0.08 μM; Imax = 50%), whereas NDNB3y showed no inhibition. None of the analogs had significant affinity for $\alpha7*$ nAChRs. Thus, unsaturated NONI analogs had enhanced affinity at $\alpha4\beta2*$- and $\alpha6\beta2*$-containing nAChRs, however a general reduction of affinity at $\alpha4\beta2*$ and an uncovering of antagonist effects at $\alpha6\beta2*$-containing nAChRs were observed with unsaturated NDNI analogs.

INTRODUCTION

Nicotine, the major alkaloid in tobacco, has intrinsic rewarding properties, which maintain chronic tobacco use and dependence.[1-3] Dopamine (DA) release evoked by nicotine via activation of presynaptic neuronal nicotinic acetylcholine receptors (nAChRs) is thought to mediate nicotine-induced reward, leading to tobacco dependence.[4-10] Mesocorticolimbic and nigrostriatal DA systems, including the nucleus accumbens, medial prefrontal cortex, and striatum have been implicated in drug-induced reward. The nucleus accumbens shell encodes primary appetitive stimuli associated with unconditioned drug reward,[11-14] including reward produced by nicotine.[5,15-17] The medial prefrontal cortex encodes secondary conditioned stimuli associated with environmental cues paired with drug, leading to reward expectancy.[14,18-21] Integration of the motivational information from medial prefrontal cortex occurs at least in part in striatum leading to initiation and execution of movement in reward expectancy and detection of reward.[22] Furthermore, nicotine dose-dependently increases neuronal activity in these brain regions in smokers, as assessed in fMRI and PET studies.[23,24]

Corresponding Author: Linda P. Dwoskin, College of Pharmacy, University of Kentucky, Lexington, KY 40536-0082. Tel: (859) 257-4743; Fax: (859) 257-7564; E-mail: ldwoskin@email.uky.edu

With varying affinity, nicotine activates all known nAChRs[25] and upon activation, nAChRs modulate the release of various neurotransmitters.[26-29] Currently available tobacco use cessation agents (ie, nicotine and bupropion) have shown limited efficacy, as relapse rates are reported to be high,[30-33] indicating a need for the development of alternative, more efficacious smoking cessation pharmacotherapies. The use of nicotine replacement as a cessation therapy is based on activation of nAChRs resulting in DA release within the relevant neural circuitry. Bupropion acts as an inhibitor of the dopamine transporter (DAT), also resulting in increased extracellular DA concentrations.[34-38] Recently, bupropion has been reported to act as a nAChR antagonist within the same concentration range that it inhibits DAT function.[38-42] Many studies have shown that nicotine-evoked DA release is completely inhibited by the classical, nonselective, noncompetitive nAChR antagonist, mecamylamine.[43-45] Mecamylamine has some efficacy as a tobacco use cessation agent, but its therapeutic use is limited by peripherally mediated side effects, eg, constipation and dry mouth.[46,47] In this respect, one therapeutic strategy is to develop novel subtype-selective nAChR antagonists that inhibit nicotine-evoked DA release in brain. Such antagonists may prove to be efficacious smoking cessation agents with fewer side effects, due to the nAChR subtype-selective action.

nAChRs are composed of 5 subunits and have been shown to have discrete expression patterns.[48-51] Genes for $\alpha2$-$\alpha7$ and $\beta2$-$\beta4$ subunits have been identified in mammalian brain.[52-55] Heteromeric nAChRs exist as combinations of α and β subunits, and variations in subunit compositions contribute to differences in nAChR function and pharmacology.[56-60] In heteromeric nAChRs, β subunits regulate the rate at which agonists and antagonists bind and dissociate from the nAChRs, as well as their pharmacological sensitivity.[61] In addition to heteromeric nAChRs, homomeric nAChRs also are present in the central nervous system, and are believed to consist of 5 $\alpha7$ subunits.[62] $\alpha4\beta2^*$ and $\alpha7^*$ nAChR subtypes are predominant in rodent brain and are probed by high-affinity binding of [^{3}H]nicotine[63-65] and [^{3}H]methyllycaconitine (MLA)[66], respectively.

nAChRs are located on DA cell bodies and terminals, including the substantia nigra and its terminal fields in striatum.[27] Substantia nigra DA neurons projecting to striatum express mRNA for $\alpha3$, $\alpha4$, $\alpha5$, $\alpha6$, $\alpha7$, $\beta2$, $\beta3$, and $\beta4$,[67-70] suggesting that variations in the combinations of these subunits may be involved in the formation of nAChR subtypes that modulate DA release at striatal presynaptic DA terminals. In this respect, the asterisk behind the nAChR subtype designation indicates the putative subunit composition of the native subtype involved in the response to nicotine.[71] Results showing that both the *Conus* snail peptide neurotoxin, α-conotoxin MII (α-CtxMII), and the small quaternary ammonium mole-

cules, *N-n*-pentadecylpyridinium bromide (NPDPB), *N-n*-eicosylpyridinium bromide (NEcPB), and *bis*-picoliniumdodecyl bromide (bPiDDB), only partially inhibit nicotine-evoked striatal [^{3}H]DA release indicate the involvement of more than one population of nAChR subtype mediating this response.[72-76]

Initially, the $\alpha3\beta2^*$ nAChR subtype was suggested to mediate nicotine-evoked striatal DA release, based on the observations that neuronal bungarotoxin and α-CtxMII were selective for the $\alpha3\beta2$ subtype in recombinant receptor assay systems[77-79] and that nicotine-evoked DA release was sensitive to inhibition by neuronal bungarotoxin and α-CtxMII.[43,72,80] Consistent with the latter results, studies using $\beta2$ knockout mice have clearly demonstrated the involvement of $\beta2$-containing nAChRs in nicotine-evoked [^{3}H]DA release.[74,81-83] However, subsequent studies with $\alpha3$ knockout and $\alpha6$ knockout mice showed that [^{125}I]α-CtxMII binding was preserved in $\alpha3$ knockout mice, but abolished in $\alpha6$ knockout mice, indicating α-CtxMII also has high affinity for $\alpha6$-containing nAChRs and that $\alpha6$-containing nAChRs mediate nicotine-evoked striatal [^{3}H]DA release.[84-86] α-CtxMII binds to critical residues that are conserved in $\alpha3$ and $\alpha6$ subunits, which are closely related.[79,87] Subsequently, Champtiaux et al[85] suggested that $\alpha4\beta2^*$, $\alpha6\beta2^*$, and $\alpha4\alpha6\beta2^*$ subtypes mediate the dopaminergic response to nicotine. $\alpha6$- and $\beta3$-containing nAChRs were also suggested to be implicated in nicotine-evoked DA release by others.[60,88] α-CtxMII was shown to bind with high affinity to immunopurified $\alpha6$- and $\beta2$-containing nAChRs, which were suggested to consist of $\alpha6\alpha2(\beta3)$ and $\alpha4\alpha6\beta2(\beta3)$ subunit compositions, whereas $\alpha4\beta2$ and $\alpha4\alpha5\beta2$ subtypes were insensitive to recognition by α-CtxMII.[89,90] Results from studies using $\beta3$-knockout mice also indicate that $\beta3$-containing nAChRs mediate α-CtxMII-sensitive nicotine-evoked DA release from striatal synaptosomes; however, compensatory increases in α-CtxMII-resistant nicotine-evoked DA release were also observed.[90] Additionally, substantia nigra neurons express high levels of both $\alpha6$ and $\beta3$ mRNA,[68,88,91,92] consistent with their involvement in mediating nicotine-evoked DA release.

Recently, a comprehensive molecular genetics study was conducted in which an individual subunit gene (ie, $\alpha4$, $\alpha5$, $\alpha7$, $\beta2$, $\beta3$, and $\beta4$) was deleted. In this study, at least 6 different nAChR subtypes were reported to mediate nicotine-evoked DA release in mouse striatal synaptosomes, including 2 classes of nAChRs: α-CtxMII-sensitive nAChRs (ie, $\alpha6\beta2\beta3^*$, $\alpha4\alpha6\beta2\beta3^*$, and possibly a small amount of $\alpha6\beta2^*$ or $\alpha4\alpha6\beta2^*$ subtypes) and α-CtxMII–resistant nAChRs (ie, $\alpha4\beta2^*$ and $\alpha4\alpha5\beta2^*$ subtypes), whereas deletion of $\beta4$ and $\alpha7$ subunits had no effect.[93] These data show that native subtypes in mouse striatum can consist of at least 5 different subunits. These different subtypes have different
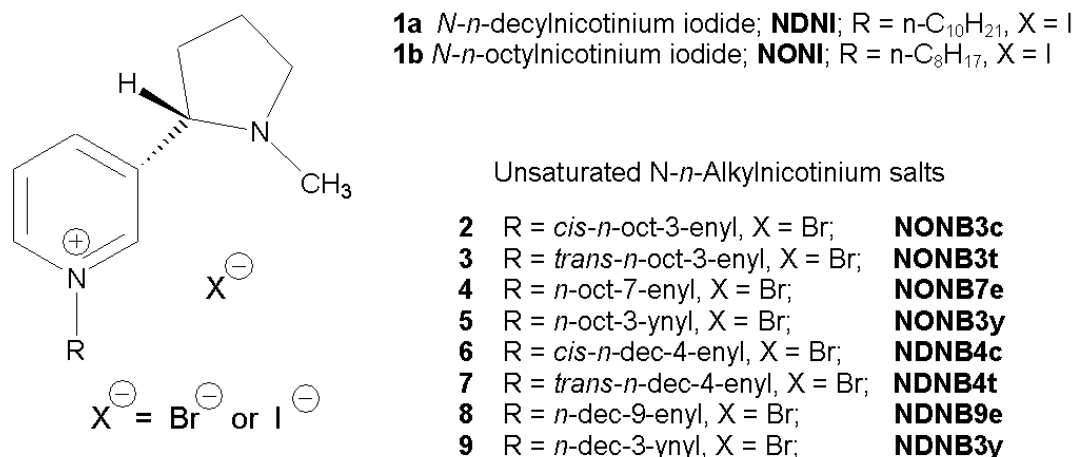
1a *N-n*-decylnicotinium iodide; **NDNI**; R = n-C$_{10}$H$_{21}$, X = I
1b *N-n*-octylnicotinium iodide; **NONI**; R = n-C$_8$H$_{17}$, X = I

Unsaturated N-*n*-Alkylnicotinium salts

2	R = *cis-n*-oct-3-enyl, X = Br;	**NONB3c**
3	R = *trans-n*-oct-3-enyl, X = Br;	**NONB3t**
4	R = *n*-oct-7-enyl, X = Br;	**NONB7e**
5	R = *n*-oct-3-ynyl, X = Br;	**NONB3y**
6	R = *cis-n*-dec-4-enyl, X = Br;	**NDNB4c**
7	R = *trans-n*-dec-4-enyl, X = Br;	**NDNB4t**
8	R = *n*-dec-9-enyl, X = Br;	**NDNB9e**
9	R = *n*-dec-3-ynyl, X = Br;	**NDNB3y**

Figure 1. Chemical structures of *N-n*-decylnicotinium iodide (NDNI; 1a); *N-n*-octylnicotinium iodide (NONI; 1b) and their unsaturated *N-n*-alkylnicotinium analogs (2–9). Chemical structure, full chemical name, and abbreviation of each unsaturated *N-n*-alkylnicotinium analog are provided.

pharmacological properties. Thus, the number of relevant nAChR subtypes involved in nicotine-evoked DA release is considerably larger than originally thought. Contemporary molecular genetics and the use of genetically engineered knockout mice, which lack one or more genes encoding specific nAChR subunits, provide a unique opportunity to analyze the pharmacology and functional role of nAChRs in a complex biological system. However, these studies have their associated limitations, in that knockout of a specific receptor subunit during development may lead to compensatory subunit combinations and the ability to provide an adaptive response, which complicates interpretation of the results.

To further complicate the association of a particular response with a specific nAChR subtype, results from recent studies using recombinant receptors have shown that when the ratio of subunit pairs is varied, different subtype classes are formed. Moreover, the function (ie, sensitivity to receptor activation, time to desensitization, and upregulation) of these different subtype classes is also dependent on subunit ratio.[94,95] Furthermore, exposure to drug (eg, nicotine) also influences nAChR subtype stoichiometry and function in recombinant receptor systems.[95,96] Evidence has also been obtained that suggests that different DA neurons in the substantia nigra can be categorized based on the expression of the specific subtype composition.[70] Thus, not only is the presence of mRNA for a particular subunit important to neuronal function and to drug response, but the relative ratio of transcribed subunits, the specific expression of nAChR subtypes by different DA neurons, and the pharmacological history of the organism also all potentially play a role in the response to nicotine.

The observation that nAChR subtypes that mediate nicotine-evoked DA release are pharmacologically different suggests that subtype-selective antagonists can be developed. As part of our drug development efforts, the nicotine molecule has been modified with the aim of obtaining subtype-selective nAChR antagonists. Simple alkylation of the pyridino *N*-atom converts S(-)-nicotine from a potent, nonselective agonist into a potent, subtype-selective, competitive antagonist.[97-99] *N-n*-Decylnicotinium iodide (NDNI; Figure 1a) potently and competitively inhibits [³H]nicotine binding and nicotine-evoked ⁸⁶Rb⁺ efflux from thalamic synaptosomes, but does not inhibit nicotine-evoked [³H]DA release.[45,100] (also Linda P Dwoskin, unpublished data, 2005) *N-n*-Octylnicotinium iodide (NONI; Figure 1b) competitively inhibits nicotine-evoked [³H]DA overflow from rat striatal slices (referred to herein as probing α6β2*-containing nAChRs), but does not inhibit [³H]nicotine binding (probing α4β2* nAChRs) to striatal membranes.[45,100] Furthermore, these analogs do not exhibit affinity for α7* nAChRs, as assessed in [³H]MLA binding assays.

The current research focuses on the development of novel, potent, and selective antagonists at nAChRs mediating nicotine-evoked DA release through structural modification of NONI and NDNI by introduction of unsaturation into the *N-n*-alkyl chain in these molecules (Figure 1). This structural change affords a novel series of unsaturated *N-n*-alkylnicotinium analogs, which were evaluated in various pharmacological assays. Analog-induced inhibition of nicotine-evoked [³H]DA overflow from superfused striatal slices assessed functional interaction at α6β2*-containing nAChRs. In this assay, DA release was determined under conditions in which the DA transporter (DAT) was blocked by nomifensine. [³H]Nicotine and [³H]MLA binding assays probed α4β2* and α7* nAChR subtypes, respectively. Analog-induced inhibition of nicotine-evoked ⁸⁶Rb⁺ efflux from thalamic synaptosomes assessed whether the analogs acted as agonists or antagonists at α4β2* nAChRs. The ability of these analogs to inhibit [³H]DA uptake into striatal synaptosomes was also determined to assess interaction with DAT.

MATERIALS AND METHODS

Chemicals

[3H]Dopamine (3,4-ethyl-2[N-3H]dihydroxyphenyl ethylamine; [3H]DA; specific activity 28.0 Ci/mmol), S-(-)-[3H]nicotine (S-(-)-[N-methyl-3H]; specific activity 81.0 Ci/mmol), and 86rubidium chloride (86RbCl; specific activity 55.2 mCi/mmol) were purchased from PerkinElmer Life Sciences Inc (Boston, MA). [3H]Methyllycaconitine ([1α,4(S),6β,14α,16β]-20-ethyl-1,6,14,16-tetramethoxy-4-[[[2-([3-3H]-methyl-2,5-dioxo-1-pyrrolidinyl)benzoyl]oxy]methyl]-aconitane-7,8-diol; [3H]MLA; specific activity 25.8 Ci/mmol) was purchased from Tocris Cookson Ltd (Bristol, UK). L-Ascorbic acid, bovine serum albumin (BSA), catechol, cesium chloride (CsCl), α-D-glucose, N-[2-hydroxyethyl] piperazine-N'-[2-ethanesulfonic acid] (HEPES), methyllycaconitine citrate (MLA), S(-)-nicotine ditartrate, nomifensine maleate, pargyline hydrochloride, sucrose, and tetrodotoxin were obtained from Sigma Chemical Co (St Louis, MO). TS-2 tissue solublizer and scintillation cocktail were purchased from Research Products International Corp (Mount Prospect, IL). All other chemicals used in buffers were purchased from Fisher Scientific (Pittsburgh, PA). The unsaturated NONI and NDNI analogs were characterized by ^{1}H and ^{13}C NMR spectroscopy, mass spectroscopy, and elemental analysis, and their synthesis was reported elsewhere.[101]

Subjects

Male Sprague-Dawley rats (200 to 225 g) were obtained from Harlan Laboratories (Indianapolis, IN) and were housed 2 per cage with free access to food and water in the Division of Laboratory Animal Resources at the College of Pharmacy, University of Kentucky. Experimental protocols involving the animals were in accordance with the NIH *1996 Guide for the Care and Use of Laboratory Animals* and were approved by the Institutional Animal Care and Use Committee at the University of Kentucky.

[3H]Nicotine Binding Assay

The [3H]nicotine binding assay was performed using a previously described method.[75,100] Briefly, striata from 2 rats were dissected, pooled, and homogenized in 10 vol of ice-cold Krebs-HEPES buffer (in mM: 20 HEPES, 118 NaCl, 4.8 KCl, 2.5 CaCl$_2$, 1.2 MgSO$_4$, pH 7.5). Homogenates were incubated at 37°C for 5 minutes, and then centrifuged (27 000*g* for 20 minutes at 4°C). Pellets were resuspended in 10 vol of ice-cold MilliQ water and incubated for 5 minutes at 37°C, followed by centrifugation (27 000*g* for 20 minutes at 4°C). The second and third pellets were resuspended in 10 vol of fresh, ice-cold 10% Krebs-HEPES buffer, incubated for 5 minutes at 37°C, and centrifuged as described above.

Final pellets were stored in 10% Krebs-HEPES buffer at –70°C until assay. During assay, the final pellets were resuspended in 20 vol of ice-cold MilliQ water, which afforded ~200 µg protein/100 µL,[102] using BSA as the standard. Binding assays were performed in duplicate in a final volume of 200 µL Krebs-HEPES buffer containing 200 mM Tris (pH 7.5 at 4°C). Assays were initiated by the addition of 100 µL of membrane suspension to assay tubes containing final concentrations of 3 nM [3H]nicotine (50 µL) and 1 of 7 concentrations of analog (0.1 nM to 100 µM; 50 µL). Nonspecific binding was defined in the presence of 10 µM nicotine (50 µL). After a 90-minute incubation at 4°C, reactions were terminated by dilution with 3 mL of ice-cold Krebs-HEPES buffer, followed immediately by filtration through Schleicher and Schuell #32 glass fiber filters (Schleicher and Schuell Inc, Keene, NH) (presoaked in 0.5% polyethylenimine [PEI], using a Brandel cell harvester [Biomedical Research and Development Laboratories, Inc, Gaithersburg, MD]). Filters were rinsed 3 times with 3 mL of ice-cold Krebs-HEPES buffer and transferred to scintillation vials, 4 mL of scintillation cocktail was added and radioactivity was determined by liquid scintillation spectroscopy (Packard model B1600 TR Scintillation Counter, Packard Instrument Co, Inc, Downer's Grove, IL).

86Rb+ Efflux Assay

To assess whether the analogs acted as agonists or antagonists at the α4β2* nAChR subtype, the 86Rb+ efflux assay was performed using a previously published method (Linda P. Dwoskin, unpublished data, 2005).[103] Thalamus was homogenized and centrifuged (1000*g*, 10 minutes, 4ºC). The supernatant fraction was centrifuged (12 000*g*, 20 minutes, 4ºC) to obtain the synaptosomal fraction. Synaptosomes were incubated for 30 minutes in 35 µL of buffer (in mM: 140 NaCl, 1.5 KCl, 2.0 CaCl$_2$, 1.0 MgSO$_4$, and 20 α–D-glucose, pH 7.5) containing 4 µCi of 86Rb+. 86Rb+ uptake was terminated by filtration of the synaptosomes onto glass fiber filters (6 mm, type A/E; Gelman Instrument Co, Ann Arbor, MI) under gentle vacuum (0.2 atm), followed by 3 washes with buffer (0.5 mL each). Subsequently, each filter with 86Rb+-loaded synaptosomes was placed on a 13-mm glass fiber filter (type A/E) mounted on a polypropylene platform. Assay buffer (in mM: 125 NaCl, 1.5 KCl, 2.0 CaCl$_2$, 1.0 MgSO$_4$, 25 HEPES, 20 α–D-glucose, and 1.0 g/L BSA, pH 7.5) was superfused at a rate of 2.5 mL/min. Tetrodotoxin (0.1 mM) and CsCl (5.0 mM) were included in the assay buffer to block voltage-gated Na+ and K+ channels, respectively, and to reduce the basal rate of 86Rb+ efflux. The ability of analog (1 nM to 100 µM) to inhibit 86Rb+ efflux evoked by 3 µM nicotine was determined. This concentration of nicotine was chosen based on initial nicotine concentration-response analysis as the lowest concentration to evoke maximal 86Rb+ efflux (EC$_{50}$ = 0.32 ± 0.08

μM, n = 7). After 8 minutes of superfusion, basal samples (sample/18s) were collected for 2 minutes. Subsequently, synaptosomes were superfused for 3 minutes in the absence or presence of 1 of 6 concentrations of analog. Then, nicotine (3 μM) was added to buffer, and superfusion was continued for an additional 3 minutes, followed by superfusion for 3 minutes with buffer in the absence of either drug. Each aliquot of thalamic synaptosomes was exposed to only one concentration of analog. In each experiment, one aliquot was also exposed to nicotine in the absence of analog, and one aliquot was superfused in the absence of either drug to determine basal ^{86}Rb$^+$ efflux. Radioactivity in superfusate and tissue samples was determined by adding 3.7 mL water to each sample, then measuring Cerenkov radiation using a scintillation counter (model B1600 TR, Packard Instrument Co, Inc, Downer's Grove, IL).

To determine the basal rate of ^{86}Rb$^+$ efflux, an exponential decay curve was used to fit the data points preceding and following superfusion with analog and nicotine (SigmaPlot 2000; SPSS, Inc, Chicago, IL). The drug-evoked increase in ^{86}Rb$^+$ efflux resulting from exposure to the analog, nicotine, or both, was calculated as the fractional increase above baseline. Increases were summed to obtain total ^{86}Rb$^+$ efflux during the period of superfusion with analog and/or nicotine, and normalized to ^{86}Rb$^+$ content in the corresponding synaptosomal sample to reduce variability within and between experiments.

[^{3}H]MLA Binding Assay

The [^{3}H]MLA binding assay was performed using previously published methods.[100] Whole rat brain minus cortex, striatum, and cerebellum, was homogenized in 20 vol of ice-cold hypotonic buffer (in mM: 2 HEPES, 14.4 NaCl, 0.15 KCl, 0.2 CaCl$_2$, and 0.1 MgSO$_4$, pH 7.5). Homogenates were incubated at 37°C for 10 minutes and centrifuged (29 000g for 17 minutes at 4°C). Pellets were washed 3 times by resuspension in 20 vol of the same buffer, followed by centrifugation using the above parameters. Final pellets were resuspended in the incubation buffer to yield ~150 μg membrane protein/100 μL membrane suspension. Binding assays were performed in duplicate, in a final volume of 250 μL of incubation buffer (in mM: 20 HEPES, 144 NaCl, 1.5 KCl, 2 CaCl$_2$, 1 MgSO$_4$, and 0.05% BSA, pH 7.5). Binding assays were initiated by the addition of 100 μL of membrane suspension to 150 μL of sample containing 2.5 nM [^{3}H]MLA and 1 of 7 concentrations of analog (1 nM to 1000 μM), and incubated for 2 hours at room temperature. Nonspecific binding was determined in the presence of 1 mM nicotine. Assays were terminated by dilution of samples with 3 mL of ice-cold incubation buffer followed by immediate filtration through Schleicher and Schuell #32 glass fiber filters (presoaked in 0.5% PEI) using the Brandel cell harvester (Biomedical

Research and Development Laboratories, Inc.). Filters were rinsed 3 times with 3 mL of ice-cold Krebs-HEPES buffer and transferred to scintillation vials, 4 mL of scintillation cocktail was added and radioactivity was determined by liquid scintillation spectroscopy (model B1600 TR Scintillation Counter, Packard Instrument Co, Inc).

[^{3}H]DA Overflow Assay

Nicotine-evoked [^{3}H]DA overflow from superfused rat striatal slices preloaded with [^{3}H]DA was determined using a previously published method.[45,75] Briefly, coronal slices of rat striata (500 μm, 6–8 mg) were obtained using a McIlwain tissue chopper (The Mickle Laboratory Engineering Co Ltd, Surrey, England). Slices were incubated for 30 minutes in Krebs' buffer (in mM: 118 NaCl, 4.7 KCl, 1.2 MgCl$_2$, 1.0 NaH$_2$PO$_4$, 1.3 CaCl$_2$, 11.1 α-D-glucose, 25 NaHCO$_3$, 0.11 L-ascorbic acid, and 0.004 ethylenediaminetetraacetic acid (EDTA), pH 7.4, saturated with 95%O$_2$/5%CO$_2$) at 34°C in a metabolic shaker. Slices were then incubated for an additional 30 minutes in fresh buffer containing 0.1 μM [^{3}H]DA. After rinsing, each slice was transferred to a glass superfusion chamber, maintained at 34°C and superfused (1 mL/min) with oxygenated Krebs' buffer containing both nomifensine (10 μM), a DA uptake inhibitor, and pargyline (10 μM), a monoamine oxidase inhibitor, ensuring that [^{3}H]overflow primarily represented [^{3}H]DA, rather than [^{3}H]metabolites.

Following superfusion for 60 minutes, three 5-minute samples (5 mL/sample) were collected to determine basal [^{3}H]outflow. After collection of the third basal sample, slices from an individual rat were superfused for 60 minutes in the absence (0 nM; control) or presence of analog (10 nM to 100 μM) to determine the intrinsic activity of the analog, ie, ability of the analog to evoke [^{3}H]overflow. Each slice was exposed to only one concentration of analog, which remained in the buffer until the end of the experiment; all concentrations of analog were exposed to striatal slices from each rat (within-subject design). Following 60 minutes of superfusion in the absence or presence of analog, nicotine (10 μM) was added to the superfusion buffer and samples were collected for an additional 60 minutes to determine the ability of the analog to inhibit nicotine-evoked [^{3}H]DA overflow. At least one striatal slice in each experiment was superfused for 60 minutes in the absence of analog, followed by superfusion with 10 μM nicotine to determine nicotine-evoked [^{3}H]DA overflow in the absence of analog (nicotine control). Using a repeated-measures design, striata from a single rat were used to determine the concentration effect of analog to release [^{3}H]DA (intrinsic activity) and to determine analog-induced inhibition of nicotine-evoked [^{3}H]DA overflow (antagonist activity).

To assess analog selectivity with respect to inhibition of the effect of nicotine, the ability of representative analogs, NDNB9e and NONB3t (0.01 µM to 1 µM) to inhibit electrical field stimulation-evoked [^{3}H]DA overflow was determined. Striatal slices were preloaded with [^{3}H]DA, as previously described. Each slice was exposed to only one concentration of analog, and superfusate samples were collected for 60 minutes. Subsequently, electrical field stimulation (1 Hz, 2 ms duration for 2 minutes; total 120 unipolar, rectangular pulses) was applied using a model SD9 stimulator (Grass Instruments, Quincy, MA). At least one control slice in each experiment was field-stimulated in the absence of analog. Superfusion continued for an additional 30 minutes. The number of electrical pulses was chosen to provide [^{3}H]DA overflow similar to that evoked by 10 µM nicotine.

After collection of the superfusate samples, the slices were retrieved from the chambers and solubilized using 1 mL of TS-2 tissue solubilizer. Scintillation cocktail (10 mL) was added to the superfusate samples. The pH and volume of the solubilized tissue samples were adjusted to that of the superfusate samples. Radioactivity in the superfusate and tissue samples was determined by liquid scintillation spectroscopy as previously described.

[^{3}H]DA Uptake Assay

The DAT inhibitor, nomifensine, was included in the superfusion buffer in [^{3}H]DA overflow assays described above, such that potential interaction of the analogs with DAT was not a factor in determining DA release. Potential interaction of the analogs with DAT was determined by evaluating the ability of the analogs to inhibit [^{3}H]DA uptake into striatal synaptosomes using a published method.[104] For each experiment, striata from an individual rat were homogenized in 20 mL of ice-cold 0.32 M sucrose containing 5 mM NaHCO$_3$ (pH 7.4) with 16 up and down strokes of a Teflon pestle homogenizer (clearance ~0.003 inches). Homogenates were centrifuged (2000g for 10 minutes at 4°C) and the resulting supernatants were again centrifuged (20 000g for 17 minutes at 4°C). Resulting pellets were resuspended in 2.4 mL of ice-cold assay buffer (in mM: 125 NaCl, 5.0 KCl, 1.5 MgSO$_4$, 1.25 CaCl$_2$, 1.5 KH$_2$PO$_4$, 10 α-D-glucose, 25 HEPES, 0.1 EDTA, 0.1 pargyline, and 0.1 ascorbic acid, saturated with 95% O$_2$/5% CO$_2$, pH 7.4). The final protein concentration was ~400 µg/mL, using BSA as the standard.[101] Assays were performed in duplicate in a total volume of 500 µL. Aliquots of synaptosomal suspension (50 µL containing 20 µg of protein) were added to tubes containing 350 µL of buffer and 50 µL of 1 of 9 concentrations of analog (final concentration, 0.01 nM to 1000 µM) and incubated at 34°C for 5 minutes. Following incubation, 50 µL of 0.1 µM [^{3}H]DA was added to the tubes and incubation continued at 34°C for 10 minutes.

Reactions were terminated by addition of 3 mL of ice-cold assay buffer. Samples were rapidly filtered through Schleicher and Schuell # 32 glass fiber filters (presoaked with 1 mM catechol buffer) using the Brandel cell harvester (Biomedical Research and Development Laboratories). Filters were subsequently washed 3 times with ice-cold assay buffer containing 1 mM catechol, transferred to scintillation vials, 10 mL of scintillation cocktail was added, and radioactivity was determined by liquid scintillation spectroscopy.

Data Analysis

For analog-induced inhibition of [^{3}H]nicotine and [^{3}H]MLA binding, data are fmoles/mg of protein and are expressed as a percentage of control, ie, specific [^{3}H]nicotine or [^{3}H]MLA binding in the absence of analog. Data were fit using a 1-site competition model, using nonlinear least-squares regression, such that $Y = Bt + (Tp - Bt)/(1 + 10^{(\log IC50 - X) n})$, where Y = specific [^{3}H]nicotine or [^{3}H]MLA binding, X = logarithm of analog concentration, Bt and Tp = minimum and maximum specific [^{3}H]nicotine or [^{3}H]MLA binding, respectively, log IC_{50} = log[analog], which decreased [^{3}H]nicotine or [^{3}H]MLA binding by 50%, and n = the pseudo-Hill coefficient. Analog affinity constants (K_i values) were calculated from IC_{50} values using the Cheng-Prusoff equation, $K_i = IC_{50}/(1 + c/K_d)$, where c is the concentration of free radioligand and K_d is the equilibrium dissociation constant of the ligand.[105]

In the [^{3}H]DA overflow assays, fractional release in each superfusate sample was calculated by dividing the [^{3}H] collected in each sample by the [^{3}H] present in the tissue at the time of sample collection. Fractional release was expressed as a percentage of total tissue tritium. Basal [^{3}H]outflow was calculated from the average fractional release in the three 5-minute samples collected prior to addition of analog to the superfusion buffer. Total [^{3}H]overflow was calculated by summing the increases of [^{3}H] above the basal [^{3}H]outflow, resulting from exposure to the analog, nicotine, or analog plus nicotine, and subtracting the basal [^{3}H]outflow for an equivalent period of analog exposure. Data were expressed as percent of control and were fitted by nonlinear, nonweighted least-squares regression using a sigmoidal function $Y = Bt + (Tp - Bt)/(1 + 10^{(\log IC50 - X)})$, where Y = total [^{3}H]overflow expressed as a percentage of nicotine-evoked response, X = logarithm of analog concentration, Bt and Tp are minimum response (held constant at 0%) and maximum response (held constant at 100%), respectively, and log IC_{50} represents the logarithm of analog concentration required to decrease nicotine (10 µM)-evoked [^{3}H]DA overflow by 50% of the maximal effect. IC_{50} values for analog-induced inhibition of nicotine-evoked [^{3}H]DA overflow were determined using an iterative nonlinear least squares curve-fitting program, PRISM version 4.0 (Graph PAD Software, Inc, San Diego, CA).
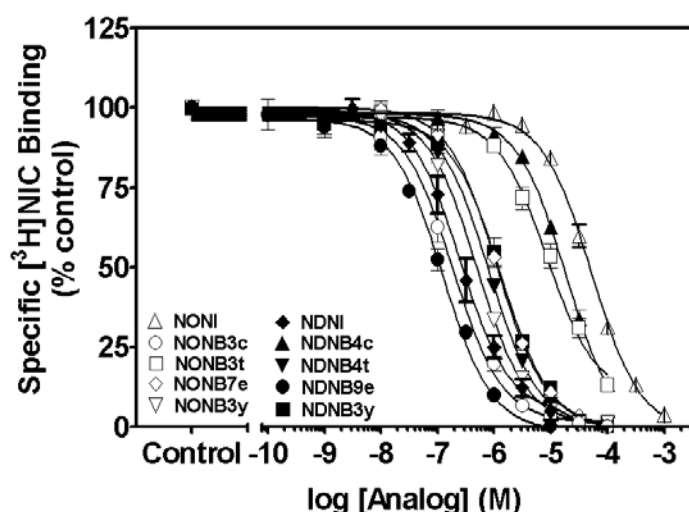
Figure 2. Unsaturated *N-n*-alkylnicotinium analogs of NONI and NDNI inhibit [³H]nicotine binding to rat striatal membranes. The ability of NONI and NDNI analogs (0.1 nM-100 µM) to inhibit [³H]nicotine binding (3 nM) was determined. Nonspecific binding was determined in the presence of 10 µM nicotine. Data are the mean ± SEM fmoles/mg of protein expressed as % of control [³H]nicotine binding for *n* = 4 rats/analog. Control is specific [³H]nicotine binding in the absence of analog (90.8 ± 1.71 fmol/mg). Curves were generated by nonlinear regression. Data for NONI and NDNI are taken from Wilkins et al.[100] Abbreviations for the analogs are defined in Figure 1. Open symbols represent NONI series analogs and closed symbols represent NDNI series analogs.

The effect of each analog on [³H]DA overflow (intrinsic activity) and its ability to inhibit nicotine-evoked [³H]DA overflow (inhibitory effect) were analyzed by 1-way repeated-measures analysis of variance (ANOVA), where concentration was a within-subjects factor (SPSS version 9.0, Chicago, IL). Where appropriate, Dunnett's *t*-tests were performed to determine the concentration of analog that either evoked [³H]DA overflow or inhibited [³H]DA overflow, compared with the respective control condition. For comparisons regarding analog intrinsic activity, the control constituted the absence of nicotine or analog (buffer control). For comparisons regarding analog-induced inhibition, the control constituted nicotine in the absence of analog (nicotine control). Additionally, a 2-way repeated-measures ANOVA was performed to analyze the time course of analog inhibition of the nicotine-evoked increase in fractional release. Both analog concentration and time were within-subjects factors. If the 2-way ANOVA revealed a significant concentration × time interaction, then 1-way repeated-measures ANOVAs were performed to determine the specific time points at which a concentration-dependent effect occurred, and Dunnett's *t*-tests were performed to determine the analog concentrations that were significantly different from the nicotine control (nicotine in the absence of analog). The ability of the analogs to inhibit electrical field stimulation-evoked [³H]DA overflow was analyzed by 1-way

repeated-measures ANOVA. Where appropriate, Dunnett's *t*-test determined significant differences between analog concentration and control (field stimulation-evoked [³H]DA overflow in the absence of analog).

For [³H]DA uptake assays, data were pmol/min/mg expressed as percentage of control ([³H]DA uptake in the absence of analog) and were fit using a 1-site competition model, and nonlinear, nonweighted least-squares regression, such that $Y = Bt + (Tp - Bt)/(1 + 10^{(\log IC_{50} - X)})$, where Y = total specific [³H]DA uptake expressed as a percentage of control, X = logarithm of analog concentration, Bt and Tp were minimum response (held constant at 0%) and maximum response (held constant at 100%), respectively. The log IC_{50}= log[analog] required to inhibit [³H]DA uptake into striatal synaptosomes by 50%. Analog affinity constants (K_i values) were calculated from IC_{50} values using the Cheng-Prusoff equation, $K_i = IC_{50}/(1 + c/K_m)$, where c is the concentration of free radioligand, K_m is concentration at which 50% of maximal velocity is achieved, and IC_{50} value represents the analog concentration inhibiting [³H]DA uptake by 50%.[105]

With respect to the ⁸⁶Rb⁺ efflux assay, both analog-induced intrinsic activity and the ability of analog to inhibit nicotine-evoked ⁸⁶Rb⁺ efflux were analyzed using 1-way repeated-measures ANOVA. Basal rate of ⁸⁶Rb⁺ efflux was determined using an exponential decay curve to fit the data points preceding and following superfusion with analog and nicotine (SigmaPlot 2000; SPSS, Inc, Chicago, IL).

RESULTS

Inhibition of [³H]Nicotine Binding

Analogs were evaluated for inhibition of [³H]nicotine binding to rat striatal membranes to determine their affinity at α4β2* nAChRs (Figure 2). In the NONI series, introduction of an unsaturated bond into the *n*-octyl chain resulted in a 4-fold to 250-fold increase in the affinity ($K_i = 0.08 - 4.49$ µM) for the [³H]nicotine binding site, when compared with the parent compound NONI ($K_i = 19.7$ µM). Furthermore, all of the compounds completely inhibited [³H]nicotine binding, with the exception of NONB3t and NDNB4c, both of which displayed 87% inhibition at the highest concentration (100 µM) tested (Figure 2). NONB3c displayed the highest affinity ($K_i = 0.08$ µM) of the analogs in the NONI series. In the NDNI series, with the exception of NDNB9e ($K_i = 0.05$ µM), affinity of the analogs for the [³H]nicotine binding site decreased 4-fold to 80-fold compared with the parent compound NDNI ($K_i = 0.09$ µM). These results demonstrate that introduction of unsaturation into the *n*-alkyl chain of NONI enhanced the affinity for α4β2* nAChR subtypes; in contrast, introduction of unsaturation into the *n*-alkyl chain of NDNI diminished affinity for α4β2* nAChRs, with the exception of NDNB9e (terminal C₉-

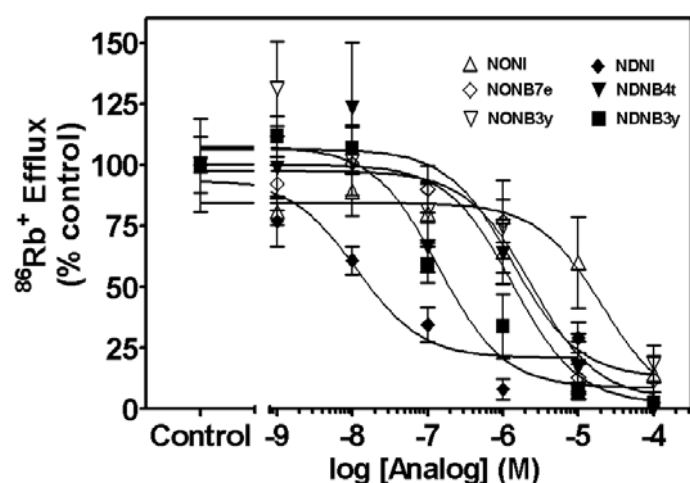**Figure 3.** Unsaturated *N-n*-alkylnicotinium analogs of NONI and NDNI inhibit nicotine-evoked ^{86}Rb$^+$–efflux from superfused rat thalamic synaptosomes. Data are presented as mean ± SEM percentage of ^{86}Rb$^+$ tissue content expressed as % of control for n = 4–7 rats/analog. Control is ^{86}Rb$^+$-efflux in response to 3 µM nicotine (0.7% ± 0.06% ^{86}Rb$^+$ tissue content) in the absence of analog. Curves were generated using nonlinear regression. Abbreviations for the analogs are defined in Figure 1. Open symbols represent NONI series analogs and closed symbols represent NDNI series analogs. Data for NONI and NDNI are taken from Wilkins et al (unpublished data, 2005).

double-bond), which showed a slight but significant increase in affinity at this site.

Inhibition of Nicotine-Evoked ^{86}Rb$^+$ Efflux

Since inhibition of [^{3}H]nicotine binding does not indicate if the analogs act as agonists or antagonists at α4β2* nAChRs, representative analogs from the NONI (ie, NONB7e and NONB3y) and NDNI (ie, NDNB4t and NDNB3y) series were investigated for their ability to induce ^{86}Rb$^+$ efflux (intrinsic agonist activity) and/or to inhibit nicotine (3 µM)-evoked ^{86}Rb$^+$ efflux from ^{86}Rb$^+$ preloaded rat thalamic synaptosomes. None of the analogs evoked ^{86}Rb$^+$ efflux above basal outflow (data not shown). In the NONI analog series, NONB7e and NONB3y inhibited nicotine-evoked ^{86}Rb$^+$ efflux (IC$_{50}$ values 2.42 and 1.66 µM, respectively), and thus, these unsaturated analogs were 3-fold to 4-fold more potent inhibitors compared with NONI (IC$_{50}$= 6.09 µM) (Figure 3). Similarly, in the NDNI series, NDNB4t and NDNB3y inhibited nicotine-evoked ^{86}Rb$^+$ efflux (IC$_{50}$= 1.21 and 0.69 µM, respectively) when compared with NDNI (IC$_{50}$ = 13.5 nM). Thus, these data demonstrate that these analogs act as antagonists at α4β2* nAChRs.

Inhibition of [^{3}H]MLA Binding

The ability of the analogs to inhibit [^{3}H]MLA binding to rat whole brain membranes is illustrated in Figure 4. Only rela-

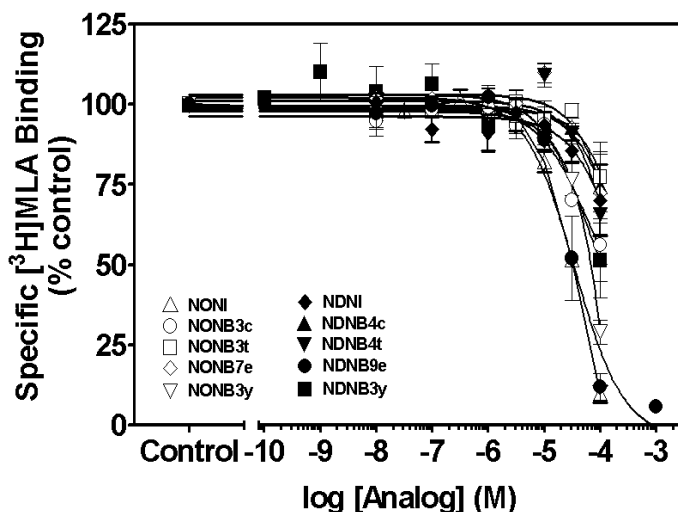**Figure 4.** High concentrations of unsaturated *N-n*-alkylnicotinium analogs of NONI and NDNI inhibit [^{3}H]MLA binding to rat whole brain membranes. The ability of *N-n*-alkylnicotinium analogs (0.1 nM-100 µM) to inhibit [^{3}H]MLA binding (2.5 nM) was determined. Nonspecific binding was determined in the presence of 1 mM nicotine. Data are mean ± SEM fmoles/mg of protein expressed as % of control [^{3}H]MLA binding for n = 3–4 rats/analog. Control represents [^{3}H]MLA binding in the absence of analog (92.9 ± 2.57 fmol/mg). Curves were generated by nonlinear regression. Data for NONI and NDNI are taken from Wilkins et al.[100] Abbreviations for the analogs are defined in Figure 1. Open symbols represent NONI series analogs and closed symbols represent NDNI series analogs.

tively high concentrations of each of the analogs in both the NONI and NDNI series inhibited [^{3}H]MLA binding. NDNB9e exhibited a K$_i$ value of 16.5 µM; however, the remaining unsaturated analogs and the parent compounds exhibited K$_i$ values greater than 100 µM, demonstrating low affinity for α7* nAChRs. Thus, introduction of unsaturation into the *n*-alkyl chain of NONI and NDNI did not improve affinity for α7* nAChRs over the parent compounds.

[^{3}H]DA Overflow: Intrinsic Activity

The ability of analogs to evoke [^{3}H]DA overflow from superfused rat striatal slices preloaded with [^{3}H]DA was determined (Table 1). One-way repeated-measures ANOVA revealed a significant effect of concentration for each analog (NONB3c, F$_{5,20}$ = 36.375, P < .001; NONB3t, F$_{5,25}$ = 37.719, P < .001; NONB7e, F$_{5,23}$ = 4344.3, P < .001; NONB3y, F$_{5,18}$ = 65.877, P < .001; NDNB4c, F$_{5,34}$ = 112.308, P < .001; NDNB4t, F$_{5,29}$ = 71.529, P < .001; NDNB9e, F$_{5,25}$ = 29.881, P < .001; NDNB3y, F$_{5,9}$ = 125.939, P < .001). Post hoc analysis revealed that the highest concentration of each analog (100 µM) evoked [^{3}H]DA overflow. In addition, each of the NDNI series of analogs evoked [^{3}H]DA overflow at 10 µM, and the parent NDNI also exhibited intrinsic activity at 1.0 µM.

Table 1. High concentrations of unsaturated *N-n*-alkylnicotinium analogs of NONI and NDNI evoke [³H]DA overflow from superfused rat striatal slices. Slices were preloaded with [³H]DA and superfused for 60 minutes with buffer containing nomifensine (10 μM) and pargyline (10 μM) to inhibit the reuptake of released [³H]DA and to prevent metabolism of [³H]DA, respectively. Subsequently, slices were superfused for 60 minutes either in the absence (control) or presence of analog, which was added to the superfusion buffer. Data represent [³H]DA overflow during the latter 60-minute period of superfusion. Each slice was exposed to only one concentration of analog. Abbreviations for the analogs are defined in Figure 1.

	Analog Concentration					
Analog	Control	0.01 μM	0.1 μM	1 μM	10 μM	100 μM
NONI[†]	0 ± 0*	0 ± 0	0 ± 0	0 ± 0	0.43 ± 0.39	25.8 ± 2.79[‡]
NONB3c	0 ± 0	0 ± 0	0 ± 0	0.08 ± 0.05	0.15 ± 0.15	10.9 ± 1.80[‡]
NONB3t	0 ± 0	0 ± 0	0 ± 0	0 ± 0	0.09 ± 0.08	9.05 ± 1.47[‡]
NONB7e	0.05 ± 0.02	0.10 ± 0.04	0.06 ± 0.04	0 ± 0	0.31 ± 0.17	18.9 ± 0.35[‡]
NONB3y	0.07 ± 0.06	0.05 ± 0.03	0.08 ± 0.03	0.14 ± 0.08	0.12 ± 0.06	22.0 ± 4.98[‡]
NDNI[†]	0.05 ± 0.04	0 ± 0	0.08 ± 0.06	3.65 ± 1.93[‡]	8.64 ± 1.06[‡]	59.2 ± 1.73[‡]
NDNB4c	0 ± 0	0 ± 0	0.08 ± 0.07	0.20 ± 0.12	8.57 ± 1.06[‡]	51.8 ± 5.31[‡]
NDNB4t	0 ± 0	0 ± 0	0 ± 0	0.32 ± 0.19	10.6 ± 0.79[‡]	59.4 ± 7.94[‡]
NDNB9e	0 ± 0	0 ± 0	0 ± 0	0 ± 0	5.86 ± 1.88[‡]	34.8± 16.6[‡]
NDNB3y	0.13 ± 0.13	0 ± 0	0.13 ± 0.08	0.09 ± 0.09	4.41 ± 0.35[‡]	30.7 ± 2.66[‡]

* Data are mean ± SEM total [³H]DA overflow expressed as a percentage of tissue tritium.

[†]Values taken from Wilkins et al.[45]

[‡]$P < .05$ different from control using Dunnett's *post hoc* comparison; n = 3–10 rats/analog.
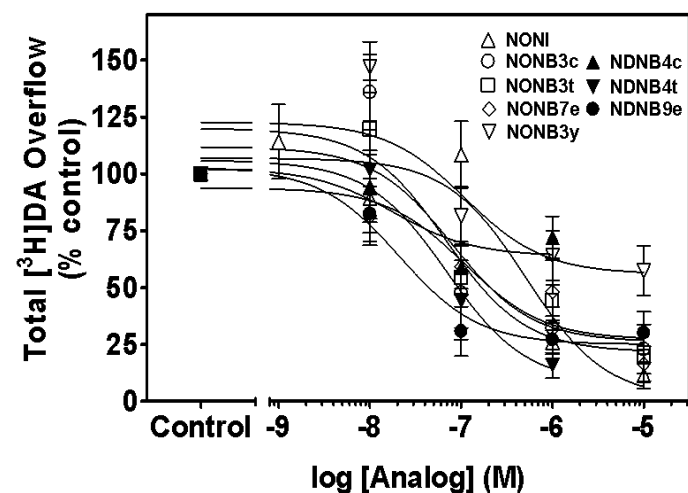

Figure 5. Unsaturated *N-n*-alkylnicotinium analogs of NONI and NDNI inhibit nicotine-evoked [³H]DA overflow from superfused rat striatal slices. Superfusion buffer contained nomifensine (10 μM) and pargyline (10 μM). Slices were superfused in the absence (control) or presence of analog for 60 minutes prior to addition of nicotine to buffer. Superfusion continued for 60 minutes with nicotine plus analog. In each experiment, at least one striatal slice was superfused with nicotine in the absence of analog (control; 3.33 ± 0.22 total [³H]DA overflow as % of tissue [³H]; mean ± SEM). Data are expressed as % of control for n = 5–7 rats/analog. Curves were generated using nonlinear regression. Data for NONI and NDNI are taken from Wilkins et al.[45] Abbreviations for the analogs are defined in Figure 1. Open symbols represent NONI series analogs and closed symbols represent NDNI series analogs.

Inhibition of Nicotine-Evoked [³H]DA Overflow

Analogs were evaluated for their ability to inhibit nicotine (10 μM)-evoked [³H]DA overflow from rat striatal slices, and the results are illustrated in Figure 5. One-way repeated-measures ANOVA revealed significant concentration-dependent inhibition for each analog (NONB3c, $F_{4,15}$ = 14.219, $P < .001$; NONB3t, $F_{4,17}$ = 19.113, $P < .001$; NONB7e, $F_{4,17}$ = 9.432, $P < .001$; NONB3y, $F_{4,12}$ = 9.552, $P < .001$; NDNB4c, $F_{3,16}$ = 4.40, $P = .015$; NDNB4t, $F_{3,13}$ = 21.861, $P < .001$; NDNB9e, $F_{3,17}$ = 13.533, $P = .001$), with the exception of NDNB3y ($F_{3,5}$ = 0.864, $P = .509$). Each of the analogs within the NONI series inhibited nicotine-evoked [³H]DA overflow (IC_{50} = 80 to 250 nM), exhibiting a 3-fold to 8-fold greater potency compared with NONI (IC_{50} = 620 nM). NONI and each of the double-bond analogs (NONB3c, NONB3t, NONB7e) exhibited a maximal effect (Imax) of 80% to 89% inhibition compared with control (nicotine-evoked [³H]DA overflow in the absence of analog). In contrast, the Imax for the triple-bond analog, NONB3y, was only 50%. Importantly, the *N-n*-decyl parent compound, NDNI, did not inhibit nicotine-evoked [³H]DA overflow (data not shown). Although NDNI had no inhibitory effect, NDNB4t and NDNB9e did inhibit nicotine-evoked [³H]DA overflow (IC_{50} = 20 to 140 nM, Imax = 84% to 88%). Furthermore, NDNB4c (IC_{50} = 80 nM) exhibited an Imax = 50%, whereas NDNB3y, similar to NDNI, showed no inhibition. The rank order of potency for the analogs to inhibit nicotine-evoked [³H]DA overflow was NDNB9e > NONB3c = NONB3t = NDNB4c > NONB3y = NDNB4t = NONB7e > NONI >>
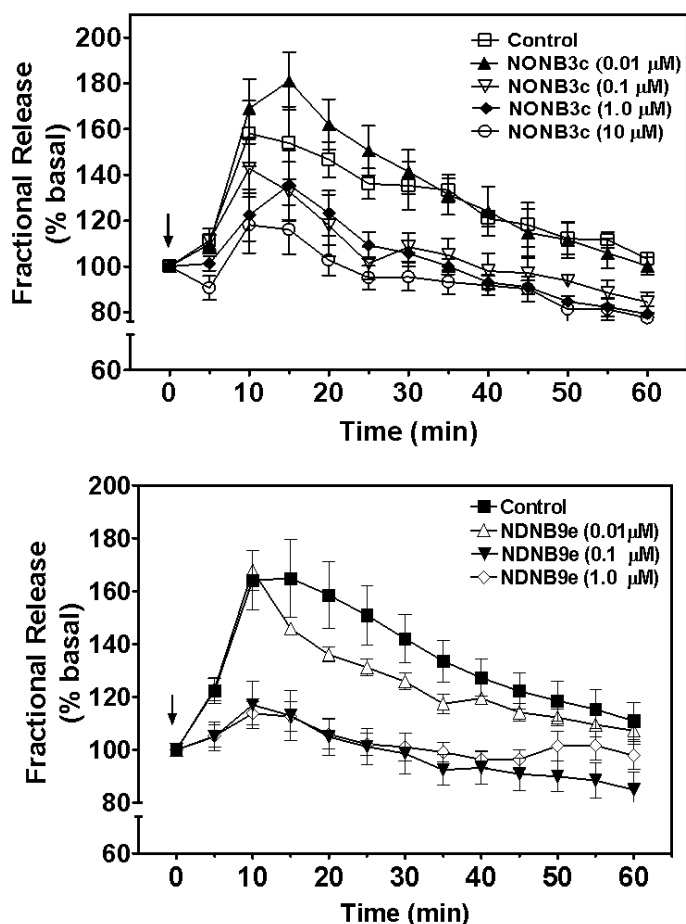
Figure 6. Time course of the inhibition induced by NONB3c (top panel) and NDNB 9e (bottom panel) on nicotine-evoked fractional [³H]DA release. Superfusion buffer contained nomifensine (10 μM) and pargyline (10 μM). Slices were superfused in the absence (control) or presence of analog for 60 minutes prior to addition of nicotine to buffer. In each experiment, one striatal slice was superfused with nicotine in the absence of analog. Data are expressed as mean ± SEM fractional DA release as a percentage of basal [³H]outflow as a function of time of superfusion (minutes) for n = 5–7 rats/analog. Arrow indicates time point of nicotine addition to the superfusion buffer. Control represents the fractional release in response to nicotine in the absence of NONB3c or NDNB9e. For the NONB3c and NDNB9e experiments, basal [³H] outflow prior to analog and/or nicotine exposure was 1.08 ± 0.06 and 0.96 ± 0.07 fractional release as a % tissue [³H], respectively. Legend provides analog concentrations.

NDNB3y = NDNI. NDNB9e was the most potent analog (IC$_{50}$ = 20 nM) to inhibit nicotine-evoked [³H]DA overflow, indicating high affinity for α6β2*-containing nAChRs.

Time courses for inhibition of the effect of nicotine exhibited by a representative analog from the NONI series, ie, NONB3c, and a representative analog in the NDNI series, ie, NDNB9e, are illustrated in Figure 6. Repeated-measures 2-way ANOVA revealed a significant concentration × time interaction for NONB3c ($F_{44,164}$ = 1.673, P = .011) and for NDNB9e ($F_{33,185}$ = 4.713, P < .001). Nicotine-evoked frac-

tional DA release peaked 10 to 15 minutes after addition of the nicotine to the buffer, and then gradually decreased toward basal levels, despite the continual presence of nicotine in the superfusion buffer throughout the remainder of the experiment. The time course also illustrates the concentration-dependent inhibition exhibited by both NONB3c and NDNB9e. Post hoc analysis revealed that 0.1 μM and 1 μM NONB3c inhibited nicotine-evoked fractional DA release from 25 to 60 minutes, and that 10 μM NONB3c inhibited the response to nicotine at 5 minutes and from 20 to 60 minutes. NDNB9e (0.1 μM) inhibited nicotine-evoked fractional DA release from 5 to 60 minutes; NDNB9e (1.0 μM) inhibited the response to nicotine from 5 to 50 minutes.

Unsaturated N-n-*Alkylnicotinium Analogs Do Not Inhibit Field Stimulation-Evoked [³H]DA Overflow*

To assess the selectivity of analog-induced inhibition of the effect of nicotine, one analog from each of the NONI and NDNI series (ie, NONB3t and NDNB9e, respectively) was evaluated for its ability to inhibit electrical field stimulation-evoked [³H]DA overflow, and the data are provided in Table 2. Striatal slices were superfused for 60 minutes in the absence (control) or presence of analog and then field stimulation was applied. One-way repeated measures ANOVA revealed that NONB3t inhibited electrically evoked [³H]DA overflow ($F_{4,14}$ = 16.376, P < .001); however, post hoc analysis revealed that significant inhibition occurred only at the highest concentration (10 μM), which is 3 orders of magnitude higher than that which inhibits nicotine-evoked [³H]DA overflow (see Table 3). Although NDNB9e tended to decease [³H]DA overflow evoked by field stimulation, the decrease did not reach significance ($F_{3,15}$ = 1.924, P = .169). Thus, the results indicate that these analogs selectively inhibit nicotine-evoked [³H]DA overflow.

Inhibition of [³H]DA Uptake

The ability of all of the NONI and NDNI analogs to inhibit [³H]DA uptake into striatal synaptosomes was determined, and the data are illustrated in Figure 7. Analogs in both the NONI and NDNI series displayed low affinity for DAT (K$_i$ = 16 to 100 μM and 2.5 to 5.3 μM, respectively), similar to NONI and NDNI (K$_i$ = 16 and 0.99 μM, respectively). Generally, the NDNI series of unsaturated analogs appeared to be more potent at inhibiting DAT function than the NONI series of unsaturated analogs. Thus, introduction of unsaturation into the *n*-alkyl chain of NONI and NDNI does not lead to enhancement of affinity for DAT.

DISCUSSION

The current study demonstrates that introduction of unsaturation into the *n*-alkyl chain of the NONI molecule enhances

Table 2. The unsaturated *N-n*-alkylnicotinium analogs, NONB3t and NDNB9e, inhibit field stimulation-evoked [^{3}H]DA overflow from superfused rat striatal slices. Superfusion buffer contained nomifensine (10 μM) and pargyline (10 μM). Slices were superfused for 60 minutes in the absence or presence of analog and then field stimulation (120 pulses, 1 Hz for 2 minutes) was applied. Superfusion continued, and samples were collected for 30 minutes. Each slice was exposed to only one concentration of analog. Control represents field stimulation-evoked [^{3}H]DA overflow in the absence of analog. Abbreviations for the analogs are defined in Figure 1.

	Analog Concentration				
Analog	**0 μM**	**0.01 μM**	**0.1 μM**	**1 μM**	**10 μM**
NONB3t	3.69 ± 0.26*	3.25 ± 0.58	2.94 ± 0.21	2.16 ± 0.65	0.05 ± 0.02‡
NDNB9e	2.61 ± 0.24	1.99 ± 0.42	1.83 ± 0.31	1.61 ± 0.17	ND†

*Data are mean ± SEM total [^{3}H]overflow expressed as a percentage of tissue tritium.

† Not determined.

‡ *P* < .05 different from 0 μM, Dunnett's test; *n* = 5–6 rats/analog.

Table 3. Summary of inhibitory activities exhibited by NONI, NDNI, and their unsaturated *N-n*-alkylnicotinium analogs

Analog	[^{3}H]NIC Binding Assay K_i (μM)	Nicotine-evoked ^{86}Rb$^+$-Efflux Assay IC$_{50}$ (μM)	[^{3}H]MLA Binding Assay K_i (μM)	Nicotine-evoked [^{3}H]DA Overflow Assay		[^{3}H]DA Uptake Assay K_i (μM)
				IC$_{50}$ (μM)	Imax (%)	
NONI	19.7 ± 2.56*,†	6.09 ± 2.51‡	23.6 ± 4.85†	0.62 ± 0.09§	89.1 ± 4.52§	15.5 ± 1.7‖
NONB3c	0.08 ± 0.009	ND¶	>100	0.08 ± 0.04	87.2 ± 4.93	>100
NONB3t	4.49 ± 0.71	ND	>100	0.09 ± 0.04	80.5 ± 2.99	>100
NONB7e	0.46 ± 0.04	2.42 ± 0.51	>100	0.25 ± 0.14	83.9 ± 7.69	15.5 ± 1.61
NONB3y	0.20 ± 0.02	1.66 ± 0.99	>100	0.13 ± 0.04	49.5 ± 11.7	28.5 ± 5.13
NDNI	0.09 ± 0.004†	0.013 ± 0.002‡	>50†	>100§	NE§,#	0.99 ± 0.05‡
NDNB4c	7.47 ± 0.37	ND	>100	0.08 ± 0.04	49.5 ± 8.59	5.27 ± 0.51
NDNB4t	0.32 ± 0.02	1.21 ± 0.81	>100	0.14 ± 0.07	87.5 ± 4.79	2.50 ± 0.84
NDNB9e	0.05 ± 0.006	ND	16.5 ± 5.27	0.02 ± 0.003	83.8 ± 6.75	4.38 ± 0.30
NDNB3y	0.57 ± 0.08	0.69 ± 0.39	>100	>100	NE	4.75 ± 0.37

*Data are mean ± SEM.

† Values taken Wilkins et al.[100]

‡ Values taken from Wilkins et al (unpublished data, 2005).

§ Values taken from Wilkins et al.[45]

‖ Values taken from Zhu et al.[103]

¶ Not determined.

No Effect; *n* = 4 rats/analog for [^{3}H]NIC binding assay; *n* = 4–7 rats/analog for ^{86}Rb-efflux assay; *n* = 3–4 rats/analog for [^{3}H]MLA binding assay; *n* = 3–5 rats/analog for [^{3}H]DA uptake assay; *n* = 3–8 rats/analog for [^{3}H]DA release assay.

affinity at both α4β2* (probed by [^{3}H]nicotine binding) and α6β2*-containing nAChRs (probed by nicotine-evoked [^{3}H]DA release); whereas introduction of unsaturation into the *n*-alkyl chain of the NDNI molecule produces mixed effects, reducing affinity at α4β2* (with the exception of NDNB9e, which was equipotent with NDNI), and uncovering an antagonist effect at α6β2*-containing nAChRs with analogs NDNB4c, NDNB4t and NDNB9e. Table 3 summarizes the affinity values for the unsaturated NONI and NDNI analogs in all of the assays evaluated in the current study. Data for the parent compounds, NONI and NDNI have been reported earlier, and show that NONI and NDNI are selective antagonists at nAChRs mediating nicotine-evoked DA release[45] and are selective ligands at the [^{3}H]nicotine binding site,[100] respectively. Specifically, NONI is a selective and competitive antagonist (IC$_{50}$ = 0.62 μM) at nAChRs mediating nicotine-evoked DA release, while exhibiting low affinity (K_i = 19.7 μM) for

[^{3}H]nicotine binding sites. In contrast, NDNI potently (K_i = 0.09 μM) and selectively inhibited [^{3}H]nicotine binding, probing α4β2* nAChR subtypes, but did not inhibit (IC$_{50}$ = >100 μM) nicotine-evoked [^{3}H]DA release.

The current study shows that in the NONI series, introduction of a C$_3$-*cis*- (NONB3c), a C$_3$-*trans*- (NONB3t), or a terminal C$_7$-double-bond (NONB7e), or a C$_3$-triple-bond (NONB3y) resulted in a 4-fold to 250-fold increase in affinity for the [^{3}H]nicotine binding site (K_i = 0.08, 4.49, 0.46, and 0.20 μM, respectively) compared with the parent compound NONI (K_i = 19.7 μM). Interestingly, there is some evidence for a geometric structural effect, since the C$_3$-*cis*-analog (NONB3c) is 60-fold more potent at the α4β2* nAChRs than the C$_3$-*trans*-analog (NONB3t). Thus, NONB3c, the most potent analog in this series, is in excess of 2 orders of magnitude greater in potency at the α4β2* nAChR than
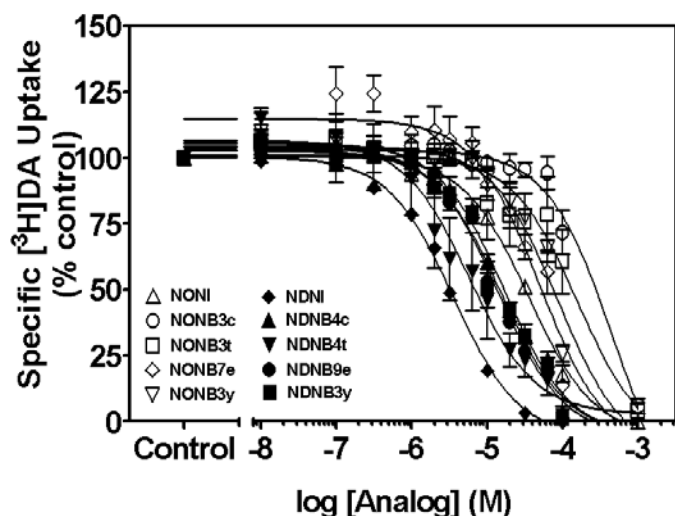
Figure 7. Unsaturated *N-n*-alkylnicotinium analogs of NONI and NDNI inhibit specific [³H]DA uptake into rat striatal synaptosomes. The ability of *N-n*-alkylnicotinium analogs (10 nM-1000 µM) to inhibit [³H]DA uptake into striatal synaptosomes was determined. Nonspecific [³H]DA uptake was determined in the presence of 10 µM nomifensine. Data are mean ± SEM picomoles/min/mg of specific [³H]DA uptake expressed as % of control [³H]DA uptake for *n* = 3–5 rats/analog. Control is specific [³H]DA uptake in the absence of analog (34.4 ± 0.94 pmol/min/mg). Curves were derived from nonlinear regression. Abbreviations for the analogs are defined in Figure 1. Data for NONI and NDNI are taken from Zhu et al.[103] Open symbols represent NONI series analogs and closed symbols represent NDNI series analogs.

NONI. Representative analogs in the NONI series, ie, NONB3y and NONB7e, inhibited nicotine-evoked $^{86}Rb^+$ efflux (K$_i$ = 1.66 and 2.42 µM, respectively), indicating that these two analogs act as α4β2* nAChR antagonists. None of the analogs in this series had significant affinity for α7* nAChRs, as probed by the [³H]MLA binding assay.

With respect to α6β2*-containing nAChRs, NONB3c, NONB3t, NONB3y, and NONB7e exhibited a 3-fold to 8-fold greater potency for inhibiting nicotine-evoked [³H]DA overflow (IC$_{50}$ = 0.08, 0.09, 0.13, and 0.25 µM, respectively) compared with NONI (IC$_{50}$ = 0.62 µM). Interestingly, there was no evidence of a geometrical isomeric effect at α6β2*-containing nAChRs, since the C$_3$-*cis*- and C$_3$-*trans*-analogs had similar potency in inhibiting nicotine-evoked [³H]DA release. Thus, introduction of unsaturation into the C$_3$ position of the *n*-alkyl chain of NONI did not alter affinity greatly. However, more importantly, introduction of a C$_3$ *cis*- or *trans*-double-bond (eg, NONB3c and NONB3t, respectively) afforded a maximal inhibition (Imax) of ~90%, whereas introduction of a C$_3$ triple bond (NONB3y) significantly reduced maximal inhibition (Imax = 50%). The current results suggest that NONB3y selectively inhibits only one subtype of nAChR mediating nicotine-evoked DA release, whereas NONB3c and NONB3t interact with more than one nAChR subtype involved in this response. The subtype-selective interaction must be related to a unique geometry of the C$_3$ triple bond analog (NONB3y), which appears to have the ability to interact with only one nAChR subtype involved in this response to nicotine. This lack of complete inhibition exhibited by some of these NONI analogs is similar to that exhibited by α-CtxMII, and the implication is that more than one nAChR subtype mediates nicotine-evoked DA release (see Introduction). However, several different subtypes may be mediating the effect of nicotine to release DA in striatum.[93] It is important to note that the previous DA release study was conducted using mouse striatal synaptosomes, whereas rat striatal slices were used in the current study. In the more intact preparations, at high micromolar concentrations of nicotine, α7* nAChRs evoke [³H]DA release via an indirect mechanism, ie, by releasing glutamate, which in turn stimulates the release of DA.[106,107] However, in the current study, unsaturated NONI analogs exhibit no interaction with [³H]MLA binding sites, suggesting that this indirect mechanism may not be involved. Thus, introduction of unsaturation into the *n*-alkyl chain of NONI afforded compounds with slightly greater potency than NONI in inhibiting nicotine-evoked DA release; however, more importantly, the introduction of a triple bond at C$_3$ afforded an analog (ie, NONB3y) that may interact with one of a subset of nAChRs mediating nicotine-evoked DA release.

NONI and its unsaturated analogs evoke DA release at a concentration of 100 µM, which is 2 to 3 orders of magnitude higher than the concentration required to inhibit nicotine-evoked DA release, indicating that these compounds are inhibitors and do not appear to act as partial agonists. Furthermore, the representative unsaturated NONI analog, NONB3t, did not inhibit electrical field stimulation–evoked DA release at concentrations less than 10 µM. Thus, NONB3t did not inhibit depolarization-induced release evoked by electrical field stimulation at concentrations that are 2 orders of magnitude lower than that which inhibits the effect of nicotine to evoke DA release. These results provide supporting evidence that the above unsaturated NONI analogs act as selective antagonists at nAChRs mediating nicotine-evoked DA release.

The DA release assay was conducted with nomifensine and pargyline included in the superfusion buffer to inhibit the reuptake and prevent the metabolism of released DA, respectively. Since DA collected in superfusate is a reflection of extracellular DA concentrations, it was considered necessary to evaluate interaction of the NONI analogs with DAT, a protein that has profound influence on extracellular DA concentrations. The current work demonstrates that none of the analogs in the NONI series had significant affinity for DAT. Thus, the results suggest that the NONI analogs inhibit

nAChRs modulating nicotine-evoked DA release, and do not alter extracellular DA concentrations via an interaction with DAT.

Table 3 also provides the results with the unsaturated analogs in the NONI series from assays probing $\alpha4\beta2^*$ and $\alpha7^*$ nAChRs. None of the unsaturated NONI analogs had appreciable affinity for $\alpha7^*$ nAChRs. NONB3c was the most potent NONI analog to inhibit [^{3}H]nicotine binding and was 2 orders of magnitude more potent than NONI. However, it is important to note that NONB3c is equipotent at both $\alpha4\beta2^*$ at $\alpha6\beta2^*$-containing nAChRs, indicating that it is not a nAChR subtype-selective agent. Similarly, NONB7e and NONB3y were 1 to 2 orders of magnitude more potent than NONI at $\alpha4\beta2^*$ nAChRs, but were equipotent at $\alpha4\beta2^*$ at $\alpha6\beta2^*$-containing nAChRs. NONB3t was 20-fold more potent than NONI at $\alpha4\beta2^*$, and was 50-fold more potent at $\alpha6$-containing nAChRs compared with $\alpha4\beta2^*$ nAChRs. Thus, introducing unsaturation into the *n*-alkyl chain of the NONI molecule afforded compounds that were more potent at $\alpha6\beta2^*$-containing nAChRs, but demonstrated less subtype selectivity.

Introduction of unsaturation into the *n*-alkyl chain of NDNI provided some unexpected findings. NDNI is a selective *N*-*n*-alkylnicotinium antagonist at $\alpha4\beta2^*$ nAChRs, since it potently inhibits [^{3}H]nicotine binding ($K_i = 0.09$ µM), but does not inhibit ($IC_{50} > 100$ µM) nicotine-evoked [^{3}H]DA release. Consistent with the results from the [^{3}H]nicotine binding assay, NDNI inhibited nicotine-evoked ^{86}Rb$^+$ efflux ($IC_{50} = 13.5$ nM), clearly indicating that NDNI acts as an antagonist at $\alpha4\beta2^*$ nAChRs (Linda P Dwoskin, unpublished data, 2005). Additionally, of all the analogs in both series, NDNI exhibited the highest affinity for DAT ($K_i = 1.0$ µM); however, similar to the NONI series compounds, NDNI has little to no affinity for $\alpha7^*$ nAChRs. None of the analogs in the unsaturated NDNI series had significant affinity for $\alpha7^*$ nAChRs. In the unsaturated NDNI series, introduction of a C_4-*cis*- (NDNB4c) or C_4-*trans*-double-bond (NDNB4t), or a C_3-triple bond (NDNB3y) resulted in a 4-fold to 80-fold decrease in affinity for the [^{3}H]nicotine binding site ($K_i = 7.47$, 0.32, and 0.57 µM, respectively) compared with NDNI ($K_i = 0.09$ µM). On the other hand, introduction of a terminal C_9 double-bond (NDNB9e) did not significantly alter affinity ($K_i = 0.05$ µM) at the $\alpha4\beta2^*$ nAChR site, but provided the most potent $\alpha4\beta2^*$ ligand in this series. Interestingly, the C_4-*trans*-analog (NDNB4t) was 20-fold more potent than the C_4-*cis*-analog (NDNB4c) in inhibiting [^{3}H]nicotine binding, demonstrating a significant geometrical isomeric effect of the C_4-double bond isomers. Representative analogs from the NDNI series (NDNB3y and NDNB4t) inhibited nicotine-evoked ^{86}Rb$^+$ efflux, indicating their action as $\alpha4\beta2^*$ nAChRs antagonists.

With respect to $\alpha6\beta2^*$-containing nAChRs, NDNI exhibited intrinsic activity at 1.0 µM, whereas a 1 order of magnitude higher concentration was required to observe intrinsic acitivty with the unsaturated analogs, suggesting that the unsaturated analogs may afford great selectivity towards inhibition. The unsaturated analogs NDNB4t and NDNB9e, which contain double bonds at the C_4 and C_9 positions of the *n*-decanyl moiety, respectively, potently inhibited nicotine-evoked [^{3}H]DA overflow ($IC_{50} = 0.14$ and 0.02 µM, respectively). This observation was surprising, and demonstrates that introduction of unsaturation into the *n*-alkyl chain of NDNI converts it from an inactive compound into the most potent $\alpha6\beta2^*$-nAChR antagonist in the series of unsaturated NDNI analogs. In contrast, introduction of a C_3 triple bond (NDNB3y) into the *n*-decanyl moiety of NDNI resulted in an inactive analog in this assay, maintaining a profile similar to NDNI. The C_4-*cis*- and C_4-*trans*-analogs of NDNI had similar potency in inhibiting nicotine-evoked [^{3}H]DA release, indicating a lack of a geometric effect at the $\alpha6\beta2^*$-containing nAChR. The finding of a C_4 geometrical isomeric effect in the [^{3}H]nicotine binding, but not in the nicotine-evoked [^{3}H]DA release assay, provides additional support that these 2 assays probe different nAChR subtypes (ie, $\alpha4\beta2^*$ and $\alpha6\beta2^*$ subtypes, respectively). Interestingly, the above analogs had significantly different Imax values in the nicotine-evoked [^{3}H]DA release assay, with the C_4 *trans*-analog (NDNB4t) affording nearly complete inhibition (Imax = 80% to 90%) and the C_4-*cis*-analog (NDNB4c) exhibiting an Imax of only 50%. Thus, the *cis* geometrical isomer appears to selectively inhibit only one nAChR subtype involved in this response, whereas the *trans*-geometrical isomer inhibits both or all subtypes involved. The current results also suggest that the *trans*-isomer inhibits the *cis*-selective subtype with the same affinity as it inhibits the other subtype(s). These structure-activity relationships (SAR) are complex and could be due to the high degree of conformational flexibility inherent in these series of compounds. Future efforts will focus on conformational preferences within these series of molecules using sophisticated molecular modeling approaches.

With respect to the selectivity of the inhibition of nicotine-evoked [^{3}H]DA release, the representative analog, NDNB9e, completely inhibited the effect of nicotine at 100 nM ($IC_{50} = 20$ nM). Importantly, NDNB9e did not significantly inhibit field stimulation–evoked [^{3}H]DA release at NDNB9e concentrations, which completely inhibited nicotine-evoked [^{3}H]DA release (Table 2 and Figure 5). NDNB9e produced 30% inhibition of field stimulation–evoked release, however this inhibition did not reach significance. Thus, in the unsaturated NDNI series, NDNB9e is the most potent analog ($IC_{50} = 20$ nM) and appears to selectivity inhibit the effect of nicotine to evoke DA release assay; however, this compound is

not nAChR subtype-selective, also being the most potent analog (K_i = 50 nM) in the [^{3}H]nicotine binding assay. Thus, NDNB9e has similar affinity at α6β2*-containing and α4β2* nAChRs subtypes.

Thus, in summary, introduction of *n*-alkyl chain unsaturation into the NONI molecule enhanced affinity at both α4β2* and α6β2*-containing nAChRs; however, a general reduction of affinity at α4β2* and an uncovering of antagonist effects at α6β2*-containing nAChRs resulted from similar modification of NDNI. Evaluation of the present structure-activity relationships reveals that the *N*-*n*-alkyl chain in the NONI and NDNI series of compounds is not producing nAChR inhibition through a physicochemical mechanism, ie, related to lipophilicity and log P (partitioning). Thus, each of the nAChR subtypes appears to be able to accommodate the *N*-*n*-alkyl substituent in a unique conformational geometry. Therefore, the conformation of the *n*-alkyl chain is an important criterion that contributes to the pharmacological activity, ie, both potency and selectivity at each of the nAChR subtypes. Thus, the availability of analogs that reflect different conformations and geometries of the *N*-*n*-alkyl substituent may afford opportunities for the development of more potent and more selective antagonists within these series of compounds, and the introduction of unsaturation into the *N*-*n*-alkyl chain is one way of providing a series of unique geometries of NONI and NDNI. These SARs are complex due to the many possible conformations that these flexible unsaturated molecules can adopt. Additional complexity arises with respect to the many potential nAChR subtypes that may be involved in nicotine-evoked DA release. Thus, the specific nAChR subtype(s) mediating nicotine-evoked DA release in the current study is not known; as a result, this complicates the drug discovery process with respect to the development of subtype-selective nAChR antagonists. To obtain a better understanding of these complex interactions, state-of-the-art molecular modeling approaches will be employed in future studies.

ACKNOWLEDGMENTS

REFERENCES

1. Clarke PB. Nicotine and smoking: a perspective from animal studies. *Psychopharmacology (Berl)*. 1987;92:135-143.

2. Pomerleau CS, Pomerleau OF. Euphoriant effects of nicotine in smokers. Euphoriant effects of nicotine in smokers. *Psychopharmacology (Berl)*. 1992;108:460-465.

3. Balfour DJ. The neurobiology of tobacco dependence: a commentary. *Respiration*. 2002;69:7-11.

4. Koob GF. Neural mechanisms of drug reinforcement. *Ann N Y Acad Sci*. 1992;654:171-191.

5. Corrigall WA, Franklin KBJ, Coen KM, Clarke PBS. The mesolimbic dopaminergic system is implicated in the reinforcing effects of nicotine. *Psychopharmacology (Berl)*. 1992;107:285-289.

6. Stolerman IP, Jarvis MJ. The scientific case that nicotine is addictive. *Psychopharmacology (Berl)*. 1995;117:2-10.

7. Pontieri F, Tanda G, Orgi F, DiChiara G. Effects of nicotine on the nucleus accumbens and similarity to those of addictive drugs. *Nature*. 1996;382:255-257.

8. Spanagel R, Weiss F. The dopamine hypothesis of reward: past and current status. *Trends Neurosci*. 1999;22:521-527.

9. Di Chiara G. Role of dopamine in the behavioural actions of nicotine related to addiction. *Eur J Pharmacol*. 2000;393:295-314.

10. Wise RA. Addiction becomes a brain disease. *Neuron*. 2000;26:27-33.

11. Wise RA, Bozarth MA. A psychomotor stimulant theory of addiction. *Psychol Rev*. 1987;94:469-492.

12. Bardo MT. Neuropharmacological mechanisms of drug reward: beyond dopamine in the nucleus accumbens. *Crit Rev Neurobiol*. 1998;12:37-67.

13. Koob GF. The role of the striatopallidal and extended amygdala systems in drug addiction. *Ann N Y Acad Sci*. 1999;877:445-460.

14. Di Chiara G, Bassareo V, Fenu S, et al. Dopamine and drug addiction: the nucleus accumbens shell connection. *Neuropharmacology*. 2004;47:227-241.

15. Fibiger HC, Phillips AG. Role of catecholamine transmitters in brain reward systems. In: Engel J, Oreland L, eds. *Brain Reward Systems and Abuse*. New York, NY: Raven Press; 1987:61-74.

16. Mansvelder HD, McGehee DS. Cellular and synaptic mechanisms of nicotine addiction. *J Neurobiol*. 2002;53:606-617.

17. Mathieu-Kia AM, Kellog SH, Butelman ER, Kreek MJ. Nicotine addiction: insights from recent animal studies. *Psychopharmacology (Berl)*. 2002;162:102-118.

18. Berridge KC, Robinson TE. What is the role of dopamine in reward: hedonic impact, reward learning, or incentive salience? *Brain Res Brain Res Rev*. 1998;28:309-369.

19. Shima K, Tanji J. Role for cingulate motor area cells in voluntary movement selection based on reward. *Science*. 1998;282:1335-1338.

20. Rose JE, Behm FM. Extinguishing the rewarding value of smoke cues: pharmacological and behavioral treatments. *Nicotine Tob Res*. 2004;6:523-532.

21. Brody AL, Mandelkern MA, Lee G, et al. Attenuation of cue-induced cigarette craving and anterior cingulate cortex activation in bupropion-treated smokers: a preliminary study. *Psychiatry Res*. 2004;130:269-281.

22. Martin-Soelch C, Leenders KL, Chevalley AF, et al. Reward mechanisms in the brain and their role in dependence: evidence from neurophysiological and neuroimaging studies. *Brain Res Brain Res Rev*. 2001;36:139-149.

23. Stein EA, Pankiewicz J, Harsch HH, et al. Nicotine-induced limbic cortical activation in the human brain: a functional MRI study. *Am J Psychiatry*. 1998;155:1009-1015.

24. Barrett SP, Boileau I, Okker J, Pihl RO, Dagher A. The hedonic response to cigarette smoking is proportional to dopamine release in the human striatum as measured by positron emission tomography and [^{11}C]raclopride. *Synapse*. 2004;54:65-71.

25. Parker MJ, Beck A, Luetje CW. Neuronal nicotinic receptor β2 and β4 subunits confer large differences in agonist binding affinity. *Mol Pharmacol*. 1998;54:1132-1139.

26. McGehee DS, Role LW. Physiological diversity of nicotinic acetylcholine receptors expressed by vertebrate neurons. *Annu Rev Physiol*. 1995;57:521-546.

27. Wonnacott S. Presynaptic nicotinic ACh receptors. *Trends Neurosci*. 1997;20:92-98.

28. Luetje CW. Getting past the asterisk: the subunit composition of presynaptic nicotinic receptors that modulate striatal dopamine release. *Mol Pharmacol*. 2004;65:1333-1335.

29. Gotti C, Clementi F. Neuronal nicotinic receptors: from structure to pathology. *Prog Neurobiol*. 2004;74:363-396.

30. Irvine JE, Hendricks PS, Brandon TH. The increasing recalcitrance of smokers in clinical trials II: pharmacotherapy trials. *Nicotine Tob Res*. 2003;5:27-35.

31. Hurt RD, Krook JE, Croghan IT, et al. Nicotine patch therapy based on smoking rate followed by bupropion for prevention of relapse to smoking. *J Clin Oncol*. 2003;21:914-920.

32. George TP, O'Malley SS. Current pharmacological treatments for nicotine dependence. *Trends Pharmacol Sci*. 2004;25:42-48.

33. Wileyto P, Patterson F, Niaura R, et al. Do small lapses predict relapse to smoking behavior under bupropion treatment? *Nicotine Tob Res*. 2004;6:357-366.

34. Richelson E, Pfenning M. Blockade by antidepressants and related compounds of biogenic amine uptake into rat brain synaptosomes: most antidepressants selectively block norepinephrine uptake. *Eur J Pharmacol*. 1984;104:277-286.

35. Nomikos GG, Damsma G, Wenkstern D, Fibiger HC. Acute effects of bupropion on extracellular dopamine concentrations in rat striatum and nucleus accumbens studied by in vivo microdialysis. *Neuropsychopharmacology*. 1989;2:273-279.

36. Ascher JA, Cole JO, Colin JN, et al. Bupropion: a review of its mechanism of antidepressant activity. *J Clin Psychiatry*. 1995;56:395-401.

37. Li SX, Perry KW, Wong DT. Influence of fluoxetine on the ability of bupropion to modulate extracellular dopamine and norepinephrine concentrations in three mesocorticolimbic areas of rats. *Neuropharmacology*. 2002;42:181-190.

38. Damaj MI, Carroll FI, Eaton JB, et al. Enantioselective effects of hydroxy metabolites of bupropion on behavior and on function of monoamine transporters and nicotinic receptors. *Mol Pharmacol*. 2004;66:675-682.

39. Fryer JD, Lukas RJ. Noncompetitive functional inhibition at diverse, human nicotinic acetylcholine receptor subtypes by bupropion, phencyclidine, and ibogaine. *J Pharmacol Exp Ther*. 1999;288:88-92.

40. Slemmer JE, Martin BR, Damaj MI. Bupropion is a nicotinic antagonist. *J Pharmacol Exp Ther*. 2000;295:321-327.

41. Miller DK, Sumithran SP, Dwoskin LP. Bupropion inhibits nicotine-evoked [(3)H]overflow from rat striatal slices preloaded with [(3)H]dopamine and from rat hippocampal slices preloaded with [(3)H]norepinephrine. *J Pharmacol Exp Ther*. 2002;302:1113-1122.

42. Gumilar F, Arias HR, Spitzmaul G, Bouzat C. Molecular mechanisms of inhibition of nicotinic acetylcholine receptors by tricyclic antidepressants. *Neuropharmacology*. 2003;45:964-976.

43. Grady SR, Marks MJ, Wonnacott S, Collins AC. Characterization of nicotinic receptor-mediated [³H]dopamine release from synaptosomes prepared from mouse striatum. *J Neurochem*. 1992;59:848-856.

44. Teng L, Crooks PA, Buxton ST, Dwoskin LP. Nicotinic-receptor mediation of S(-)-nornicotine-evoked [³H]-overflow from rat striatal slices preloaded with [³H]-dopamine. *J Pharmacol Exp Ther*. 1997;283:778-787.

45. Wilkins LH, Haubner A, Ayers JT, Crooks PA, Dwoskin LP. *N-n*-Alkylnicotinium analogs, a novel class of nicotinic receptor antagonist: Inhibition of S(-)-nicotine-evoked [³H]dopamine overflow from super-fused rat striatal slices. *J Pharmacol Exp Ther*. 2002;301:1088-1096.

46. Rose JE, Behm FM, Westman EC, Levin ED, Stein RM, Ripka GV. Mecamylamine combined with nicotine skin patch facilitates smoking cessation beyond nicotine patch treatment alone. *Clin Pharmacol Ther*. 1994;56:86-99.

47. Rose JE, Westman EC, Behm FM, Johnson MP, Goldberg JS. Blockade of smoking satisfaction using the peripheral nicotinic antagonist trimethaphan. *Pharmacol Biochem Behav*. 1999;62:165-172.

48. Anand R, Conroy WG, Schoepfer R, Whiting P, Lindstrom J. Neuronal nicotinic acetylcholine receptors expressed in *Xenopus* oocytes have a pentameric quaternary structure. *J Biol Chem*. 1991;266:11192-11198.

49. Cooper E, Couturier S, Ballivet M. Pentameric structure and subunit stoichiometry of a neuronal nicotinic acetylcholine receptor. *Nature*. 1991;350:235-238.

50. Boorman JP, Groot-Kormelink PJ, Sivilotti LG. Stoichiometry of human recombinant neuronal nicotinic receptors containing the β3 subunit expressed in Xenopus oocytes. *J Physiol*. 2000;529:565-577.

51. Perry DC, Xiao Y, Nguyen HN, Musachio JL, Davila-Garcia MI, Kellar KJ. Measuring nicotinic receptors with characteristics of alpha4beta2, alpha3beta2 and alpha3beta4 subtypes in rat tissues by autoradiography. *J Neurochem*. 2002;82:468-481.

52. Le Novere N, Changeux JP. Molecular evolution of the nicotinic acetylcholine receptor: an example of multigene family in excitable cells. *J Mol Evol*. 1995;40:155-172.

53. Lindstrom J. Neuronal nicotinic acetylcholine receptors. In: Narahashi T, ed. *Ion Channels,* vol. 4. New York, NY: Plenum Press;1996:377-450.

54. Lindstrom J. The structures of neuronal nicotinic receptors. In: Clementi F, Fornasari D, Gotti C, eds. *Handbook of Experimental Pharmacology: Neuronal Nicotinic Receptors,* vol. 144. Berlin, Germany: Springer; 2000:101-162.

55. Elgoyhen AB, Vetter DE, Katz E, Rothlin CV, Heinemann SF, Boulter J. α10: a determinant of nicotinic cholinergic receptor function in mammalian vestibular and cochlear mechanosensory hair cells. *Proc Natl Acad Sci USA*. 2001;98:3501-3506.

56. Luetje CW, Patrick J. Both alpha and beta-subunits contribute to the agonist sensitivity of neuronal nicotinic acetylcholine receptors. *J Neurosci*. 1991;11:837-845.

57. Harvey SC, Luetje CW. Determinants of competitive antagonist sensitivity on neuronal nicotinic receptorß subunits. *J Neurosci*. 1996;16:3798-3806.

58. Ramirez-Latorre J, Yu CR, Qu X, Perin F, Karlin A. Functional contributions of α5 subunit to neuronal acetylcholine receptor channels. *Nature*. 1996;380:347-351.

59. Chavez-Noriega LE, Crona JH, Washburn MS, Urrutia A, Elliott KJ, Johnson EC. Pharmacological characterization of recombinant human neuronal nicotinic acetylcholine receptors hα2β2, hα2β4, hα3β2, hα3β4, hα4β2, hα4β4 and hα7 expressed in Xenopus oocytes. *J Pharmacol Exp Ther*. 1997;280:346-356.

60. Kuryatov A, Olale F, Cooper J, Choi J, Lindstrom J. Human α6 subtypes: subunit composition, assembly and pharmacological responses. *Neuropharmacology*. 2000;39:2570-2590.

61. Papke RL. The kinetic properties of neuronal nicotinic receptors: genetic basis of functional diversity. *Prog Neurobiol*. 1993;41:509-531.

62. Sgard F, Charpantier E, Bertrand S, et al. A novel human nicotinic receptor subunit, α10 that confers functionality to the α9-subunit. *Mol Pharmacol*. 2002;61:150-159.

63. Whiting P, Schoepfer R, Lindstrom J, Priestley T. Structural and pharmacological characterization of the major brain nicotinic acetyl-choline receptor subtype stably expressed in mouse fibroblasts. *Mol Pharmacol*. 1991;40:463-472.

64. Flores CM, Rogers SW, Pabreza LA, Wolfe BB, Kellar KJ. A subtype of nicotinic cholinergic receptor in rat brain is composed of α4 and β2 subunits and is up-regulated by chronic nicotine treatment. *Mol Pharmacol*. 1992;41:31-37.

65. Peng X, Gerzanich V, Anand R, Whiting PJ, Lindstrom J. Nicotine-induced increase in the neuronal nicotinic receptors results from a decrease in the rate of receptor turnover. *Mol Pharmacol*. 1994;46:523-530.

66. Davies AR, Hardick DJ, Blagbrough IS, Potter BV, Wolstenholme AJ, Wonnacott S. Characterization of the binding of [^{3}H]methyllycaconi-tine: a new radioligand for labeling α7-type neuronal nicotinic acetyl-choline receptors. *Neuropharmacology*. 1999;38:679-690.

67. Wada E, Wada K, Boulter J, et al. Distribution of alpha 2, alpha 3, alpha 4 and beta 2 neuronal nicotinic receptor subunit mRNAs in the central nervous system: A hybridization histochemical study in the rat. *J Comp Neurol*. 1989;284:314-335.

68. Deneris ES, Boulter J, Swanson LW, Patrick J, Heinemann S. β3: a new member of nicotinic acetylcholine receptor gene family is expressed in brain. *J Biol Chem*. 1989;264:6268-6272.

69. Klink R, d'Exaerde AA, Zoli M, Changeux JP. Molecular and physi-ological diversity of nicotinic acetylcholine receptors in the midbrain dopaminergic nuclei. *J Neurosci*. 2001;21:1452-1463.

70. Azam L, Winzer-Serjhan UH, Chen Y, Leslie FM. Expression of neu-ronal nicotinic acetylcholine receptor subunit mRNAs within midbrain dopamine neurons. *J Comp Neurol*. 2002;444:260-274.

71. Lukas RJ, Changeux JP, Le Novere N, et al. International Union of Pharmacology. XX. Current status of the nomenclature for nicotinic acetylcholine receptors and their subunits. *Pharmacol Rev*. 1999;51:397-401.

72. Kulak JM, Nguyen TA, Olivera BM, McIntosh JM. Alpha-conotoxin MII blocks nicotine-stimulated dopamine release in rat striatal synapto-somes. *J Neurosci*. 1997;17:5263-5270.

73. Kaiser SA, Soliakov L, Harvey SC, Luetje CW, Wonnacott S. Differential inhibition by α-conotoxin-MII of the nicotinic stimulation of [^{3}H]dopamine release from rat striatal synaptosomes and slices. *J Neurochem*. 1998;70:1069-1076.

74. Grady SR, Meinerz NM, Cao J, et al. Nicotine agonists stimulate acetylcholine release from mouse interpeduncular nucleus: a function mediated by a different nAChR than dopamine release from striatum. *J Neurochem*. 2001;76:258-268.

75. Grinevich VP, Crooks PA, Sumithran SP, Haubner AJ, Ayers JT, Dwoskin LP. *N-n*-Alkylpyridinium analogs, a novel class of nicotinic receptor antagonists: selective inhibition of nicotine-evoked [^{3}H]dopamine overflow from superfused rat striatal slices. *J Pharmacol Exp Ther*. 2003;306:1011-1020.

76. Dwoskin LP, Sumithran SP, Zhu J, Deaciuc AG, Ayers JT, Crooks PA. Subtype-selective nicotinic receptor antagonists: potential as tobacco use cessation agents. *Bioorg Med Chem Lett*. 2004;14:1863-1867.

77. Luetje CW, Wada K, Rogers S, et al. Neurotoxins distinguish between different neuronal nicotinic acetylcholine receptor subunit com-binations. *J Neurochem*. 1990;55:632-640.

78. Cartier GE, Yoshikami D, Gray WR, Luo S, Olivera BM, McIntosh JM. A new α-conotoxin which targets α3β2 nicotinic acetylcholine receptors. *J Biol Chem*. 1996;271:7522-7528.

79. Harvey SC, McIntosh JM, Cartier GE, Maddox FN, Luetje CW. Determinants of specificity for α-conotoxin MII on α3β2 neuronal nico-tinic receptors. *Mol Pharmacol*. 1997;51:336-342.

80. Schulz DW, Zigmond RE. Neuronal bungarotoxin blocks the nico-tinic stimulation of endogenous dopamine release from rat striatum. *Neurosci Lett*. 1989;98:310-316.

81. Picciotto MR, Zoli M, Rimondini R, et al. Acetylcholine receptors containing the β2 subunit are involved in the reinforcing properties of nicotine. *Nature*. 1998;391:173-177.

82. Whiteaker P, Marks MJ, Grady SR, et al. Pharmacological and null mutation approaches reveal nicotinic receptor diversity. *Eur J Pharmacol*. 2000;393:123-135.

83. Grady SR, Murphy KL, Cao J, Marks MJ, McIntosh JM, Collins AC. Characterization of nicotinic agonist-induced [^{3}H]dopamine release from synaptosomes prepared from four mouse brain regions. *J Pharmacol Exp Ther*. 2002;301:651-660.

84. Champtiaux N, Han ZY, Bessis A, et al. Distribution and pharmacol-ogy of alpha 6-containing nicotinic acetylcholine receptors analyzed with mutant mice. *J Neurosci*. 2002;22:1208-1217.

85. Champtiaux N, Gotti C, Cordero-Erausquin M, et al. Subunit compo-sition of functional nicotinic receptors in dopaminergic neurons investi-gated with knock-out mice. *J Neurosci*. 2003;23:7820-7829.

86. Whiteaker P, Peterson CG, Xu W, et al. The role of the α3 subunit in neuronal nicotinic biding populations. *J Neurosci*. 2002;22:2522-2529.

87. McIntosh JM, Azam L, Staheli S, et al. Analogs of α-conotoxin MII are selective for α6-containing nicotinic acetylcholine receptors. *Mol Pharmacol*. 2004;65:944-952.

88. Le Novere N, Zoli M, Changeux JP. Neuronal nicotine receptor α6 subunit mRNA is selectively concentrated in catecholaminergic nuclei of the rat brain. *Eur J Neurosci*. 1996;8:2428-2439.

89. Zoli M, Moretti M, Zanardi A, McIntosh JM, Clementi F, Gotti C. Identification of the nicotinic receptor subtypes expressed on dopaminer-gic terminals in the rat striatum. *J Neurosci*. 2002;22:8785-8789.

90. Cui C, Booker TK, Allen RS, et al. The β3 nicotinic receptor subunit: a component of α-conotoxin MII-binding nicotinic acetylcholine recep-tors that modulate dopamine release and related behaviors. *J Neurosci*. 2003;23:11045-11053.

91. Goldner FM, Dineley KT, Patrick JW. Immunohistochemical local-ization of the nicotinic acetylcholine receptor subunit α6 to dopaminergic neurons in the substantia nigra and ventral tegmental area. *Neuroreport*. 1997;8:2739-2742.

92. Charpantier E, Barneoud P, Moser P, Besnard F, Sgard F. Nicotinic acetylcholine subunit mRNA expression in dopaminergic neurons of the rat substantia nigra and ventral tegmental area. *Neuroreport*. 1998;9:3097-3101.

93. Salminen O, Murphy KL, McIntosh JM, et al. Subunit composition and pharmacology of two classes of striatal presynaptic nicotinic acetyl-choline receptors mediating dopamine release in mice. *Mol Pharmacol*. 2004;65:1526-1535.

94. Zwart R, Vijverberg HP. Four pharmacologically distinct subtypes of alpha4beta2 nicotinic acetylcholine receptor expressed in *Xenopus laevis* oocytes. *Mol Pharmacol*. 1998;54:1124-1131.

95. Lopez-Hernandez GY, Sanchez-Padilla J, Ortiz-Acevedo A, et al. Nicotine-induced upregulation and desensitization of α4β2 neuronal nicotinic receptors depend on subunit ratio. *J Biol Chem*. 2004;279:38007-38015.

96. Nelson ME, Kuryatov A, Choi CH, Zhou Y, Lindstrom J. Alternate stoichiometries of alpha4beta2 nicotinic acetylcholine receptors. *Mol Pharmacol*. 2003;63:332-341.

97. Crooks PA, Ravard A, Wilkins LH, Teng LH, Buxton ST, Dwoskin LP. Inhibition of nicotine-evoked [^{3}H]dopamine release by pyridino *N*-substituted nicotine analogues: a new class of nicotinic antagonist. *Drug Dev Res*. 1995;36:91-102.

98. Dwoskin LP, Xu R, Ayers JT, Crooks PA. Recent developments in neuronal nicotinic acetylcholine receptor antagonists. *Exp Opin Ther Pat*. 2000;10:1561-1581.

99. Dwoskin LP, Crooks PA. Competitive neuronal nicotinic receptor antagonists: a new direction for drug discovery. *J Pharmacol Exp Ther*. 2001;298:395-402.

100. Wilkins LH, Grinevich VP, Ayers JT, Crooks PA, Dwoskin LP. *N-n*-Alkylnicotinium analogs, a novel class of nicotinic receptor antagonists: interaction with α4β2* and α7* neuronal nicotinic receptors. *J Pharmacol Exp Ther*. 2003;304:400-410.

101. Crooks PA, Xu R, Sumithran SP, Deaciuc AG, Dwoskin LP. NONI and NDNI analogs: structural modification of the *N-n*-alkyl moiety and the effect on neuronal nicotinic receptor activity. *Bioorg Med Chem*. 2005.

102. Bradford MM. A rapid and sensitive method for the quantitation of microgram quantities of protein utilizing the principle of protein-dye binding. *Anal Biochem*. 1976;72:248-254.

103. Miller DK, Crooks PA, Dwoskin LP. Lobeline inhibits nicotine-evoked [^{3}H]dopamine overflow from rat striatal slices and nicotine-evoked ^{86}Rb$^+$ efflux from thalamic synaptosomes. *Neuropharmacology*. 2000;39:2654-2662.

104. Zhu J, Crooks PA, Ayers JT, Sumithran SP, Dwoskin LP. *N-n*-Alkylnicotinium and *N-n*- alkylpyridinium analogs inhibit the dopamine transporter: Selectivity as nicotinic receptor antagonists. *Drug Dev Res*. 2003;60:270-284.

105. Cheng Y, Prusoff WH. Relationship between the inhibition constant (Ki) and the concentration of inhibitor which causes 50 percent inhibition (I$_{50}$) of an enzymatic reaction. *Biochem Pharmacol*. 1973;22:3099-3108.

106. McGehee DS, Heath MJ, Gelber S, Devay P, Role LW. Nicotinic enhancement of fast excitatory synaptic transmission in CNS by presy-naptic receptors. *Science*. 1995;269:1692-1696.

107. Kaiser SA, Wonnacott S. α-Bungarotoxin-sensitive nicotinic receptors indirectly modulate [^{3}H]dopamine release in rat striatal slices via glutamate release. *Mol Pharmacol*. 2000;58:312-318.